International Journal of Nanomedicine

Dovepress
Taylor & Francis Group

Open Access Full Text Article

REVIEW

Gold Nanoplatforms for Phenotypic Reprogramming and Closed-Loop Theranostics of Cancer Stem Cells

Bingyan Zhu[1–4], Yuling Chen[1–4], Yuntao Lin[1–4], Tingting Luo[1–4], Hongyu Yang[1–4], Bo Lin[1–4]

[1]Department of Oral and Maxillofacial Surgery, Stomatological Center, Peking University Shenzhen Hospital, Shenzhen, Guangdong, 518036, People's Republic of China; [2]Guangdong Province Engineering Research Center of Oral Disease Diagnosis and Treatment, Shenzhen, Guangdong, 518036, People's Republic of China; [3]The Institute of Stomatology, Peking University Shenzhen Hospital, Shenzhen Peking University-The Hong Kong University of Science and Technology Medical Center, Shenzhen, Guangdong, 518036, People's Republic of China; [4]Shenzhen Clinical Research Center for Oral Diseases, Shenzhen, Guangdong, 518036, People's Republic of China

Correspondence: Bo Lin, Department of Oral and Maxillofacial Surgery, Stomatological Center, Peking University Shenzhen Hospital, Guangdong Provincial High-Level Clinical Key Specialty, No. 1120 Lianhua Road, Futian District, Shenzhen, Guangdong, 518036, People's Republic of China, Email amber001@pku.org.cn

Abstract: Conventional physical interventions, including static photothermal ablation, frequently fail to eradicate cancer stem cells (CSCs) and instead induce sublethal stress that promotes therapeutic resistance. To address this translational challenge, this review establishes a comprehensive framework utilizing engineered gold nanoplatforms to advance the treatment strategy from non-specific cytotoxicity toward mechanism-driven phenotypic reprogramming. We outline how stimuli-responsive surface functionalization helps resolve the size-permeability paradox to secure precise intracellular access. Upon internalization, these platforms suppress intrinsic defenses by intercepting morphogenic pathways, inducing mesenchymal-to-epithelial transitions, and disrupting the bioenergetic dependence of multidrug resistance. Following this phenotypic stabilization, gold nanostructures catalyze targeted cell death via ferroptotic redox disruption and dual-metabolic blockade, alongside the immunological remodeling of the tumor microenvironment. Ultimately, by integrating real-time metabolic feedback with macroscopic surveillance, this strategy highlights the potential of gold nanoplatforms as adaptive, responsive systems to achieve precision therapy and overcome CSC-driven relapse.

Keywords: cancer stem cells, gold nanoparticles, phenotypic reprogramming, closed-loop theranostics, tumor microenvironment

Introduction

Clinical control of malignant tumors remains limited by the persistence of cancer stem cells (CSCs). As a distinct tumor-initiating population, CSCs drive metastasis, treatment relapse, and multidrug resistance (MDR)[1,2] Common cytotoxic treatments rarely eliminate CSCs completely. These treatments often enrich tumors with resistant phenotypes. Resistant CSCs avoid death through quiescence (G_0/G_1 phase), enhanced drug efflux via ATP-binding cassette (ABC) transporters, and robust DNA damage repair (DDR) pathways.[3,4]

CSCs also show high phenotypic plasticity. Epithelial-mesenchymal transition (EMT) and metabolic reprogramming help CSCs survive single-target therapies. Developing therapeutic strategies that dismantle multilayered CSC defenses has become a key goal in modern oncology.

Effective treatment requires platforms that combine physical cytotoxicity with precise biochemical regulation. Gold nanoparticles (AuNPs) are promising tools due to their unique physicochemical properties. First, the high atomic number of gold (Z=79) boosts local radiation effects through the Auger effect. This produces complex DNA double-strand breaks that outpace the DDR capacity of radioresistant CSCs.[4,5] Second, the tunable localized surface plasmon resonance (LSPR) of AuNPs supports photothermal therapy (PTT). PTT lowers intracellular ATP levels and weakens energy-dependent ABC transporters. This process reverses efflux-mediated drug resistance.[6]

https://doi.org/10.2147/IJN.S606614
Received: 3 March 2026
Accepted: 17 June 2026
Published: 3 July 2026

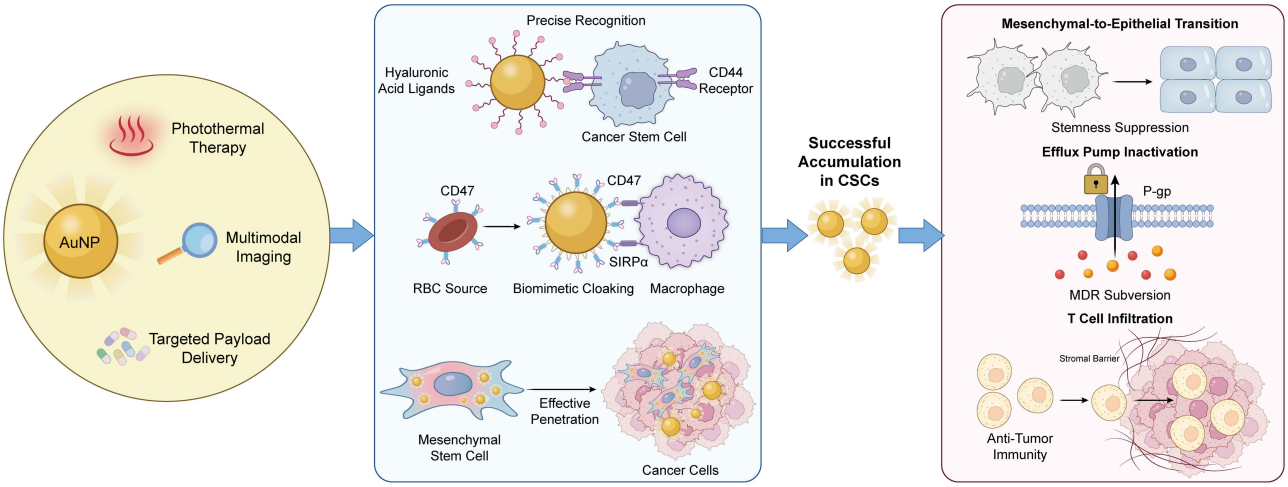

Figure 1 Nanoscale Engineering and Synergistic Delivery Network for CSC Targeting. This schematic illustrates the conceptual framework of engineered gold nanoplatforms for counteracting cancer stem cell malignant phenotypes. The diagram highlights three core integrated functionalities: photothermal therapy, targeted payload delivery, and multimodal imaging. Key approaches incorporate hyaluronic acid ligand targeting for precise recognition, erythrocyte membrane biomimetic camouflage for prolonged circulation, and mesenchymal stem cell carriers for enhanced tumor homing. These synergistic strategies enable the systematic suppression of core CSC traits, including stemness maintenance, multidrug resistance, and immune evasion.

Abbreviations: AuNP, gold nanoparticle; CSC, cancer stem cell; RBC, red blood cell; SIRPα, signal regulatory protein alpha; P-gp, P-glycoprotein; MDR, multidrug resistance.

AuNPs also enable dense conjugation of targeting ligands such as hyaluronic acid (HA). These ligands bind strongly to CD44 and other CSC markers. This improves receptor-mediated uptake and disrupts focal adhesion dynamics. Such effects block CSC retention in protective niches.[7,8]

A large gap remains between preclinical potential and clinical application. Most translational efforts focus heavily on physical ablation while ignoring adaptive biological responses of CSCs.[5] Sustained thermal stress triggers protective survival pathways. These include upregulation of heat shock proteins (HSP70/90) and shifts toward antioxidant synthesis such as hypotaurine. These changes foster a thermotolerant phenotype.[9,10]

In physiological environments, protein corona formation can mask surface ligands and reduce targeting precision. The immunosuppressive tumor microenvironment (TME) also shields residual CSCs. CD47 overexpression is one key protective mechanism.[11,12] Durable tumor control requires a shift from simple physical ablation to comprehensive phenotypic reshaping. In this framework, AuNP systems simultaneously disrupt stemness signaling, reverse metabolic adaptations, and remodel the immune microenvironment.

This review builds a functional link between nanoscale material design and the biological control of CSC-driven malignancy. Rather than summarizing general synthetic methods, we analyze how AuNPs act as a multi-mechanistic network to overcome CSC defenses. We outline three core intervention areas: molecular reprogramming, in which AuNPs mediate epigenetic modulation and gene silencing to induce CSC differentiation;[13,14] microenvironmental remodeling, which emphasizes immunogenic cell death (ICD) induction and reversal of immunosuppressive niches through HSP inhibition and CD47 blockade;[11] and theranostic integration, which uses the optical properties of AuNPs for real-time monitoring of intracellular redox metabolites to confirm therapeutic activation.[10,15] We also evaluate key translational challenges including protein corona interference and tumor heterogeneity, and propose mechanism-driven solutions to guide next-generation CSC-targeted nanomedicine. The overall structure of this nanotherapeutic framework is illustrated in Figure 1.

Spatiotemporal Control of Nanotherapeutic Delivery

Effective targeting and elimination of CSCs require therapeutic carriers to cross a series of physiological barriers. These barriers separate the administration site from deeply located, often hypoxic, tumor niches. Ideal delivery systems need

long systemic circulation to utilize the enhanced permeability and retention (EPR) effect. They must also extravasate into dense tumor interstitium. AuNPs offer a rigid scaffold that meets these conflicting needs.

Unlike soft organic carriers such as liposomes, the metallic core of AuNPs supports stable high-density ligand modification via gold-thiol chemistry.[16] This physicochemical stability allows the design of hierarchical systems. These systems remain intact in the bloodstream but respond dynamically to the tumor microenvironment.

The Size-Permeability Paradox at the Bio-Nano Interface

Interactions between AuNPs and biological environments follow strict physicochemical rules, where particle size directly determines biodistribution and cellular internalization kinetics. Empirical data show that AuNPs with diameters between 20–50 nm provide optimal tumor accumulation, limiting rapid renal clearance seen in particles below 10 nm and reticuloendothelial system (RES) sequestration seen in particles larger than 200 nm.[7,12] A critical paradox arises in CSC targeting, however. Intermediate-sized particles support strong passive accumulation via the EPR effect, but often lack sufficient diffusivity to penetrate the dense extracellular matrix surrounding CSC clusters or cross the nuclear pore complex for epigenetic regulation. In contrast, ultra-small particles that enable deep tissue penetration and nuclear entry are prone to fast pharmacokinetic elimination and potential off-target toxicity, such as undesired mesenchymal differentiation.[17]

To resolve these opposing design requirements, recent approaches have turned to multistage delivery systems with stimuli-responsive size transformation. In this design, AuNPs are first formed into larger supramolecular assemblies or polymer-coated structures for systemic transport, ensuring long circulation and reduced renal filtration. Upon exposure to TME-specific stimuli including acidic pH or overexpressed matrix metalloproteinases, these assemblies disassemble in a controlled manner to release small, highly-penetrating AuNP cores.[18,19] This size-shrinkable strategy uses gold surface engineering to separate circulation requirements from penetration requirements. Moreover, surface modification with hydrophilic polymers such as polyethylene glycol or zwitterionic ligands is critical to reduce protein corona formation. This biological adsorption layer can otherwise mask targeting ligands and change the nanoparticle's synthetic identity, leading to non-specific uptake by phagocytes rather than receptor-mediated endocytosis by CSCs.[11,20] The biological identity of nanocarriers also changes dynamically under real physiological conditions. As shown by Salvati et al, protein coronas formed in complex human serum—rather than standard in vitro media—rapidly block active ligands including transferrin, highlighting the need for dynamic cloaking strategies.[21] Therefore, rational AuNP design must move past static size optimization and emphasize dynamic adaptability to overcome physical barriers in the CSC niche.[22]

Surface Architectonics and Biomimetic Camouflage

While physical dimensions govern initial biodistribution, the final behavior of AuNPs in biological systems is determined by their surface physicochemical properties. Unlike soft organic carriers, the gold core provides a stable platform for precise surface engineering through high-affinity gold-sulfur coordination bonds. This stable interface supports the construction of molecular logic gates that convert environmental signals into controlled therapeutic responses. Stimuli-responsive polymers or HA shells can be attached to the gold surface to perform Boolean AND logic, where cargo release or ligand exposure only occurs under specific external triggers.

Successful layer-by-layer assembly of these gated structures is commonly verified by surface characterization methods, especially sequential changes in zeta potential during functionalization. Stepwise shifts in surface charge confirm the deposition of intermediate layers and the formation of a negatively charged HA outer layer, providing reliable evidence for structural stability and modification efficiency.[23] For example, AuNPs coated with hyaluronidase-sensitive or reductively cleavable shells remain intact during blood circulation but break down in response to enzyme-rich or high-glutathione conditions in the tumor microenvironment.[22,24] This stimuli-responsive shedding exposes inner targeting ligands to enhance uptake and can also reduce particle size, converting larger assemblies into ultra-small units for deeper penetration into dense extracellular matrix.[25]

To further improve targeting specificity and avoid immune clearance, surface design has advanced from synthetic polymer modification to biomimetic camouflage. Although PEGylation reduces protein adsorption, it may trigger anti-PEG antibodies and limit long-term application. Coating AuNPs with natural cell membranes has therefore become

a more effective strategy. Membranes from erythrocytes or platelets transfer a series of surface antigens, including the anti-phagocytic marker CD47, which binds to signal regulatory protein alpha (SIRPα) on phagocytes and suppresses clearance.[26,27] Recent studies have developed hybrid membrane coatings that combine the long-circulation trait of erythrocytes and tumor-homing ability of platelets, effectively separating biological navigation from the therapeutic function of the nanoparticle core.[28,29]

Even advanced surface coatings still depend on passive diffusion or blood flow for delivery. To overcome these limitations, cell-mediated delivery uses living cells as active carriers. Mesenchymal stem cells and macrophages naturally migrate toward hypoxic and inflammatory regions, enabling them to deliver internalized AuNPs across barriers inaccessible to passive nanocarriers.[30,31] Although premature exocytosis remains a challenge, modified macrophages with suppressed exocytic pathways have been developed to retain payloads until reaching the target site.[32] The evolution from chemically programmed logic gates to living biohybrid systems represents the current frontier in bypassing multiple barriers of the CSC niche.

Logic-Gated Target Recognition

Although surface engineering improves systemic circulation, single-receptor targeting remains limited by heterogeneous marker expression and off-target uptake in normal tissues. Stemness-related receptors such as CD44 and HER2 are also present in normal somatic stem cells and epithelial tissues, leading to unavoidable off-target interactions. To address this problem, nanocarrier design has shifted from simple active targeting to logic-gated recognition. This approach uses Boolean AND logic, where therapeutic activation only occurs when two distinct conditions are satisfied simultaneously: the presence of specific surface antigens and a unique intracellular or microenvironmental state. This dual-validation mechanism keeps the payload inactive until a CD44-positive malignant phenotype is confirmed.

The specificity of CD44-mediated uptake has been rigorously verified using endocytosis inhibitors, CD44 knockdown and competitive blocking assays to confirm pathway dependence.[9,33] The most direct application of this strategy is dual-ligand modification to enhance binding avidity only on cells co-expressing two markers. For instance, gold nanorods conjugated with both HA and anti-HER2 antibodies can distinguish CSCs from cells expressing only one receptor.[34] Similarly, manganese-doped mesoporous silica-gold vehicles modified with folic acid and HA enable simultaneous targeting of folate receptor-positive cancer cells and CD44-positive CSC subsets, expanding therapeutic coverage while preserving specificity.[35]

In addition to spatial recognition, advanced AuNP systems integrate biochemical responsiveness to achieve functional AND logic. In this design, the surface ligand acts as the first recognition unit, and a CSC niche-specific enzyme or metabolite serves as the second trigger. A typical example is using HA not only as a targeting ligand but also as a protective gating shell. After internalization by CD44-positive cells, the HA shell is degraded by intracellular hyaluronidase, which is highly upregulated in tumor lysosomes.[22,36] Importantly, the gold core acts as an energy acceptor through Nanometal Surface Energy Transfer (NSET), keeping attached photosensitizers quenched and inactive. Enzymatic cleavage breaks this energy transfer by separating the payload from the core, structurally and photophysically activating the system.[37]

Recent progress has extended these logic gates to target the unique metabolic profile of tumors. Janus gold-mesoporous silica nanoparticles functionalized with lactate oxidase can sense the Warburg effect. In this system, high local lactate levels trigger hydrogen peroxide production, which induces cleavage of phenylboronate caps and drug release.[38] This metabolic gating can be combined with gene silencing. For instance, AuNPs delivering siRNA against heat shock protein 72 (HSP72) sensitize tumor cells to photothermal therapy. The dual-condition requirement is met only when the cell binds the CD44-targeted particle and undergoes photothermal heating under HSP72 suppression, thereby overcoming thermotolerance.[9] These multi-input systems mark a shift from passive accumulation to active biological computation at the nanoscale.

Intrinsic Phenotypic Reprogramming of Cancer Stem Cells

Precise intracellular delivery represents a fundamental prerequisite for effective CSC targeting. However, the accumulation of therapeutic agents within tumor tissues is frequently compromised by the intrinsic plasticity of CSCs. This

subpopulation evades conventional cytotoxicity through a multidimensional defense network, including the maintenance of cellular quiescence, the upregulation of drug efflux transporters, and the dynamic modulation of metabolic pathways. Overcoming these biological barriers requires a paradigm shift from passive cargo accumulation to active phenotypic reprogramming.

This strategy utilizes the catalytic and physicochemical properties of gold nanostructures to directly intervene in the epigenetic and metabolic checkpoints that sustain stemness. By driving resistant tumorigenic cells toward a differentiated and therapy-sensitive phenotype, this approach reduces the therapeutic threshold and sensitizes malignant populations for sustained tumor suppression.[1,2] Within this framework, phenotypic reprogramming defines the dynamic biological process of promoting cellular differentiation, whereas phenotypic locking describes the stable state in which phenotypic reversion is actively prevented.

Epigenetic Remodeling and Transcriptional Modulation

Epigenetic plasticity enables CSCs to dynamically switch between dormant and proliferative states through a complex interplay of histone modifications and RNA methylation. While traditional small-molecule inhibitors often exhibit limited bioavailability, AuNPs act as intrinsic epigenetic modulators that interact with intracellular redox and chaperone networks to reshape the chromatin landscape. Although the key evidence for these epigenetic and epitranscriptomic effects derives mainly from bulk tumor populations, such findings offer a robust theoretical framework for designing targeted CSC therapies.

Recent studies using near-infrared responsive quinacrine-gold hybrid nanoparticles show that these constructs inhibit the nuclear translocation of HSP70. This inhibition dysregulates the HSP70–P300 complex and leads to a specific reduction in histone H3K14 acetylation.[39] Since H3K14 acetylation is critical for maintaining an open chromatin structure at oncogenic loci, its suppression downregulates stemness-driving factors including TGF-β and promotes cells to exit their undifferentiated state. Importantly, comparative epigenetic analyses confirm that this dysregulated H3K14 acetylation is unique to breast CSCs, indicating these nanoplatforms cause minimal epigenetic disruption in normal somatic stem cells.[39]

Beyond chromatin architecture, the epitranscriptomic control of mRNA stability via N6-methyladenosine modification serves as a post-transcriptional checkpoint for CSC maintenance. This intervention relies on the high affinity of gold surfaces for thiols. Upon internalization, AuNPs function as potent scavengers that undergo surface ligand exchange with intracellular GSH. This reaction depletes nuclear and cytosolic antioxidant pools and disrupts the reducing environment required for the activity of iron-dependent m6A demethylases such as FTO and ALKBH5.[13]

The oxidative stress caused by GSH depletion oxidizes the essential ferrous cofactor to its ferric state and inactivates these demethylases. This blockade prevents the removal of methylation marks and leads to a global increase in RNA methylation on transcripts of pluripotency factors including *SNAI1* and *MYC*, as well as the cystine/glutamate antiporter *SLC7A11*. These hypermethylated transcripts are subsequently recognized by YTHDF reader proteins and targeted for rapid degradation, silencing the genetic programs that sustain self-renewal while simultaneously weakening the antioxidant defenses needed to resist ferroptosis.[13,40]

Intercepting Morphogenic Signaling Pathways

Following epigenetic remodeling, the second stage of intrinsic reprogramming demands the blockade of upstream signaling cascades. Among the complex networks regulating cellular plasticity, the morphogenic triad of Wnt/β-catenin, Notch, and Hedgehog (Hh) acts as the primary regulatory hub for CSC self-renewal and therapeutic resistance. Although small-molecule inhibitors targeting these pathways exist, their clinical utility is often limited by poor aqueous solubility and off-target toxicity. Gold-based nanoplatforms address these pharmacological limitations through signal interception, using dense surface functionalization to disrupt these pathways at both receptor and transcriptional levels.

The Wnt/β-catenin pathway functions as a fundamental driver of stemness and requires strong suppression to achieve phenotypic locking. Unlike soft organic carriers, the rigid AuNP core supports high-density, oriented antibody conjugation via robust thiol chemistry, maximizing receptor avidity for efficient blockade. Recent bioengineering strategies

leverage this physicochemical advantage to create combinational gold nanoshells that target the pathway at multiple levels.

By conjugating antibodies against Frizzled-7 (FZD7) and loading siRNA against β-catenin, these constructs achieve a dual-inhibitory effect: the antibody physically blocks the receptor to prevent ligand binding, while the siRNA mediates post-transcriptional silencing. This synergistic intervention significantly downregulates downstream targets such as Axin2 and c-Myc and effectively arrests cells in a non-proliferative state.[14,41] Furthermore, the protein corona formed on AuNPs can be engineered to stabilize hydrophobic Wnt antagonists such as PKF118-310, facilitating their intracellular delivery.[20]

Parallel to Wnt, the Notch signaling pathway acts as a critical sensor of the hypoxic niche. Targeting this mechanism requires systems capable of simultaneous metabolic and signaling modulation. Folic acid-functionalized gold nanoclusters encapsulated within polymeric carriers have been designed to co-deliver gliotoxin, a fungal metabolite that targets the Notch cascade. These carriers effectively penetrate the hypoxic tumor core and downregulate key Notch components including Notch1 and Hes1, while concurrently reducing HIF-1α expression. By disrupting the hypoxia-Notch axis, the nanocarriers sensitize triple-negative breast cancer cells to therapy and inhibit the formation of secondary mammospheres.[42,43]

Finally, the Hh pathway, regulated by the Gli1 transcription factor, acts as a key driver of multidrug resistance. Spherical nucleic acids (SNAs), consisting of a gold core densely functionalized with siRNA, offer a highly efficient architecture for silencing these targets compared with linear oligonucleotides. By targeting Gli1, these SNAs effectively reduce the expression of downstream drug efflux transporters such as ABCG2. The dense radial arrangement of oligonucleotides on the gold surface facilitates scavenger receptor-mediated uptake and protects the siRNA cargo from nuclease degradation.

This precise interception leads to the downregulation of resistance genes and sensitizes resistant neurospheres to chemotherapeutics including temozolomide[44] or doxorubicin.[45] This collective blockade of morphogenic signaling networks renders the CSC population vulnerable to subsequent metabolic or oxidative interventions.

Phenotypic Locking via MET Induction

Blocking upstream morphogenic signaling triggers the regression of the mesenchymal program and drives a mesenchymal-to-epithelial transition (MET). This biological process converts highly motile cells into a stationary epithelial phenotype, thereby lowering metastatic potential and drug resistance. AuNPs support this phenotypic reversion by destabilizing core transcriptional repressors that maintain the mesenchymal state. It is important to note that while these transition dynamics have been verified mainly in heterogeneous bulk tumor models, they represent a highly translatable strategy for restricting CSC plasticity.

This transcriptional regulation also acts on the PI3K/AKT signaling axis, which is critical for preserving the undifferentiated state. Low-dose PEGylated AuNPs combined with cold plasma inhibit PI3K/AKT activation and reduce the secretion of pro-invasive factors. This treatment downregulates zinc-finger transcription factors including Slug and Zeb1, leading to a significant drop in sphere-forming efficiency and self-renewal capacity in glioblastoma models.[46] In addition, biosynthesized gold nanoparticles selectively target the $CD44^{+}/CD24^{-}$ stem-like subpopulation in head and neck squamous cell carcinoma. By suppressing Snail and Twist1 expression, these nanoparticles cause a dose-dependent reduction in the stem-like cell fraction and weaken the aggressive phenotype linked to tumor recurrence.[47] Furthermore, integrating targeted gold nanostars with specific differentiation agents such as retinoic acid can actively force breast CSCs to exit their self-renewing state, as evidenced by the profound depletion of ALDH-positive subpopulations and the suppression of tumorsphere formation.[48]

In line with these observations, studies in pancreatic adenocarcinoma and melanoma show that AuNPs prevent chemotherapy-induced mesenchymal transition by preserving the membrane localization of E-cadherin and lowering vimentin expression.[49,50] This structural stabilization sensitizes resistant cell populations to standard treatments by strictly limiting their phenotypic plasticity.[51]

Bioenergetic Subversion of Multidrug Resistances

Based on the phenotypic stabilization achieved through MET, engineered AuNPs offer a strong bioenergetic strategy to overcome multidrug resistance (MDR). Instead of targeting the active sites of ABC transporters, these platforms deplete the cellular ATP pool and cut off the energy supply required for efflux function. Although the basis of this metabolic disruption was established mainly in non-stem bulk tumor cells, exploiting these bioenergetic weaknesses provides a reliable translatable method to disable the efflux machinery in CSCs.

This metabolic blockade mainly targets the mitochondrial respiration pathway. Specific amino-functionalized AuNPs selectively accumulate inside the mitochondrial matrix, driven by negative membrane potential, and disrupt the electron transport chain. The resulting loss of membrane potential sharply reduces intracellular ATP levels. The causal relationship between nanoparticle-induced ATP depletion and transporter dysfunction is strongly supported by direct intracellular ATP luminescence measurements. In addition, early studies confirm that efflux activity can be partially restored by exogenous ATP supplementation, offering clear evidence for the energy-dependent nature of this blockade.[52]

Alongside this direct respiratory disruption, bioenergetic subversion works synergistically with mild hyperthermia. Photothermal treatment using gold nanocages inhibits upstream transcriptional activators including heat shock factor 1 and mutant p53, thereby downregulating the *MDR1* gene and reducing P-gp expression at the transcriptional level.[53]

Beyond metabolic interference, AuNP carriers use spatial avoidance to bypass membrane transporters. Unlike free therapeutic molecules that are quickly pumped out, drug-loaded gold nanocrystals or nanogels enter cells via receptor-mediated endocytosis and release their payloads deep inside the endolysosomal system. This physically separates drugs from membrane-bound efflux pumps.[54,55] Advanced hierarchical platforms, such as double-metal hybrid systems, combine this physical bypass with redox disruption. This multimodal network actively suppresses stemness markers including Nanog and Sox2, overcoming MDR through simultaneous bioenergetic and spatial modulation.[56]

Targeted Execution and Metabolic Vulnerabilities

After neutralizing intrinsic resistance pathways ranging from epigenetic plasticity to multidrug efflux, CSCs become phenotypically stable but remain biologically viable. For maximal therapeutic effect, the strategy must shift from phenotypic modulation to active cellular clearance. Importantly, gold nanoplatforms do not follow a single unified cell death pathway. Instead, the induction of ferroptosis, apoptosis or other death programs depends strongly on surface functionalization and the baseline redox state of the local tumor microenvironment.

In this execution phase, gold nanostructures move beyond passive carriers to act as catalytic nanoreactors. By exploiting the fragile redox balance and iron dependence of sensitized CSCs, AuNPs actively disrupt cellular bioenergetic infrastructure and drive cells toward regulated cell death.

Ferroptotic Nanoreactors and Redox Disruption

Ferroptosis acts as a major effector mechanism in this nanotherapeutic framework by triggering iron-dependent lipid peroxidation. CSCs normally maintain strong antioxidant defenses through the SLC7A11/GPX4 axis, but engineered AuNPs can overcome these protections via a synergistic triad: antioxidant depletion, intracellular labile iron mobilization, and catalytic ROS amplification. Although the detailed ferroptotic cascades were first defined in non-stem bulk cancer cells, applying these redox interventions offers a rational approach to breaking the unique metabolic defenses of CSCs.

Building on the epigenetic silencing of SLC7A11 described earlier, the first step involves direct depletion of the remaining GSH pool. Because GSH is an essential cofactor for repairing lipid peroxidation, specialized gold nanoclusters use high-affinity gold–sulfur interactions to bind and eliminate intracellular GSH, weakening the cellular reducing capacity.

Recent designs further enhance this effect by integrating redox-active components. For example, core–shell composite nanoparticles sustain GSH depletion through redox cycling of cerium oxidation states, while also inducing mitochondrial dysfunction via zinc ion overload.[57] Similarly, GSH-bioimprinted gold nanocomposites selectively target leukemic stem cells to disrupt redox balance, causing GPX4 inactivation and lipid peroxide accumulation.[13]

After antioxidant depletion, the gold surface promotes hydroxyl radical production through Fenton-like chemistry, converting endogenous H_2O_2 into strong oxidative mediators. Advanced DNA origami-based nanoreactors spatially organize AuNPs and iron oxide nanoclusters to form an enzymatic cascade. This platform sequentially generates H_2O_2 via glucose oxidase-like activity and converts it to hydroxyl radicals through peroxidase-like activity.[58] In addition, multicomponent systems such as trimetallic nanoplatforms incorporate nitric oxide donors. In these designs, the acidic microenvironment triggers breakdown of the outer shell to deplete GSH, while the released iron core catalyzes the Fenton reaction to establish a self-amplifying oxidative stress loop.[59,60]

Ultimately, oxidative stress is further strengthened by mobilization of the intracellular labile iron pool. Certain gold–polyherbal conjugates induce ferritinophagy, degrading ferritin to release stored iron and fuel the ferroptotic cascade.[61] This is supported by strategies using salinomycin-loaded AuNPs, which sequester iron in lysosomes and inhibit GPX4 to overcome baseline ferroptosis resistance.

Although some hybrid configurations can also activate intrinsic apoptosis,[62] ferroptosis dominates in these targeted models, as confirmed experimentally. Early studies showed that cell viability could be effectively restored by specific ferroptosis inhibitors such as ferrostatin-1, while apoptosis inhibitors including Z-VAD-FMK had little effect.[63] Together, these mechanisms confirm that AuNPs act directly to disrupt the metabolic stability of CSCs.

Dual-Blockade of Tumor Energetics

While ferroptosis destabilizes the lipidome, residual CSCs often survive via metabolic plasticity. Unlike differentiated tumor cells that mainly depend on aerobic glycolysis (the Warburg effect), CSCs can switch flexibly between glycolysis and oxidative phosphorylation (OXPHOS) to adapt to energy stress. Single-pathway inhibition is therefore not sufficient; full suppression requires simultaneous dual blockade of cytosolic and mitochondrial energy production. Gold nanostructures with organelle-targeting ability enable this bioenergetic disruption by delivering inhibitors that systematically damage the respiratory machinery.

The first intervention targets glycolytic dependence in CSCs by blocking nutrient uptake and initial phosphorylation. Conventional inhibitors often show poor pharmacokinetic properties, but gold nanocarriers permit precise delivery to the tumor niche. For example, gold nanorods modified with HA and diclofenac (DC) are designed to target the CD44 receptor. After internalization, released DC downregulates glucose transporter 1 (Glut1), cutting off the main carbon source of the cell.

This glucose restriction initiates a metabolic cascade that lowers intracellular ATP and suppresses HSP70 and HSP90 synthesis, thereby sensitizing thermotolerant CSCs to later photothermal ablation.[6] In parallel with transport inhibition, direct blockade of hexokinase 2 (HK2)—the rate-limiting enzyme of glycolysis—is achieved using mitochondria-targeted gold nanoparticles loaded with 3-bromopyruvate (3-BP). By delivering 3-BP directly to the outer mitochondrial membrane, these nanoconstructs dissociate HK2 from the voltage-dependent anion channel (VDAC).

This separation not only stops glycolytic flux but also triggers opening of the mitochondrial permeability transition pore, promoting cytochrome c release and apoptosis.[64,65]

To block metabolic escape through mitochondrial respiration, the second step of this strategy involves direct physical disruption of the OXPHOS machinery. Gold nanostars modified with the pro-apoptotic peptide TPP-KLA are engineered to target mitochondria specifically. The triphenylphosphonium (TPP) group drives accumulation inside the mitochondrial matrix against the membrane potential, while the KLA peptide destroys mitochondrial membrane integrity.

This physical perforation dissipates the proton gradient required for ATP synthase activity, effectively halting oxidative phosphorylation. When combined with doxorubicin, this system produces a coordinated effect: energy-dependent drug efflux pumps are inactivated by ATP depletion, trapping the chemotherapeutic agent inside the nucleus.[66]

In addition, the dynamic metabolism of CSCs requires real-time monitoring to detect adaptive resistance. The inherent plasmonic properties of gold allow the use of surface-enhanced Raman scattering (SERS) to track metabolic changes in situ. Recent studies have used gold nanostructures to visualize the accumulation of hypotaurine, a cysteine-derived antioxidant metabolite that rises in glioblastoma under hypoxic stress.

By identifying such metabolic signatures, AuNPs act as both therapeutic agents and diagnostic probes, enabling early detection of metabolic escape before clinical relapse occurs.[10] This integration of glycolytic inhibition, mitochondrial disruption and metabolic imaging forms a complete strategy to overcome the bioenergetic flexibility of CSCs.

Overcoming Intrinsic Thermotolerance

While metabolic treatments disrupt bioenergetic stability, the therapeutic effect of PTT is often limited by the intrinsic heat shock response. To reduce this thermotolerance, engineered AuNPs use a pre-sensitization strategy that pharmacologically or transcriptionally inhibits HSP70 and HSP90 before thermal stimulation. This intervention converts thermotolerance to thermosensitivity, allowing mild-temperature PTT to induce apoptosis. Although these thermal pre-sensitization approaches have been mainly tested in heterogeneous bulk tumors, applying these chaperone inhibitory mechanisms provides a strong mechanistic basis for overcoming the intrinsic thermotolerance of CSCs.

Recent bioengineering strategies use broad metabolic suppression to lower the thermal threshold. Since molecular chaperones need large amounts of ATP to maintain protein stability, glucose restriction acts as an effective upstream inhibitor. Multifunctional gold nanorods modified with glucose oxidase and HA actively consume intratumoral glucose to suppress ATP production, which in turn prevents stress-induced upregulation of HSP90α and HSP70.

The resulting proteotoxic stress makes CD44-overexpressing cells much more sensitive to mild hyperthermia.[67] Alternatively, direct pharmacological inhibition is achieved using gold–MnO_2 nanoprobes combined with the HSP90 inhibitor ganetespib. The manganese dioxide shell relieves tumor hypoxia to improve photodynamic efficacy, while released ganetespib disrupts the HSP90 chaperone complex to greatly reduce thermal resistance.[68]

Beyond chaperone regulation, PTT-induced proteotoxic stress triggers the unfolded protein response in the endoplasmic reticulum, activating the JNK pathway and upregulating markers including CHOP and Ero1Lα. This stress signal induces a protective autophagic response marked by autophagolysosome formation to support cell survival.[69]

To counter this survival pathway, autophagy inhibitors are directly incorporated into nanoplatforms. Albumin-modified gold nanorods co-delivering hydroxychloroquine block autophagic flux, leading to the accumulation of p62 protein and significantly reduced clonogenicity in neuroblastoma stem cells.[70] Furthermore, near-infrared irradiation of quinacrine–gold hybrid nanoparticles simultaneously inhibits HSP70 expression and destroys mitochondrial membrane potential, shifting cell death from autophagy-dependent survival to apoptosis.[71]

To summarize these interventions, Figure 2 shows the intracellular cascade from morphogenic signaling inhibition to bioenergetic and chaperone suppression, and Table 1 lists the molecular targets and corresponding synergistic strategies that collectively disrupt the CSC survival network.

The Durability and Reversibility of Phenotypic Locking

While engineered AuNPs can effectively restrict CSC plasticity, it is critical to assess the long-term stability of this effect. A key question in translational research is whether phenotypic reversion (including MET) represents stable terminal differentiation or only temporary stress adaptation. Emerging evidence indicates that some phenotype switches induced by nanotherapeutics act as survival responses to acute physical or oxidative damage.[72] In such cases, morphological changes reflect adaptive stress rather than permanent cellular reprogramming.

This transient behavior creates a high risk of phenotypic relapse. Once nanotherapy-induced stress is relieved—through nanoparticle exocytosis, degradation or dilution after cell division—the suppressed CSC population can rapidly recover mesenchymal and tumorigenic properties. Basic studies of CSC dynamics confirm that pharmacological inhibition of stemness and sphere formation is highly reversible after treatment withdrawal.[73] This reversibility reveals a major flaw in current ablation-focused strategies: they often fail to erase intrinsic cancer cell memory maintained by mechanotransduction and epigenetic marking in the TME.[74]

True phenotypic locking therefore requires nanomaterials to not just trigger transient oxidative stress, but to stably and permanently reprogram deep epigenetic and transcriptional cancer cell memory. Future nanoplatforms must shift from acute cytotoxicity to long-term epigenetic modulation, ensuring that the induced epithelial state is stably embedded in cellular identity.

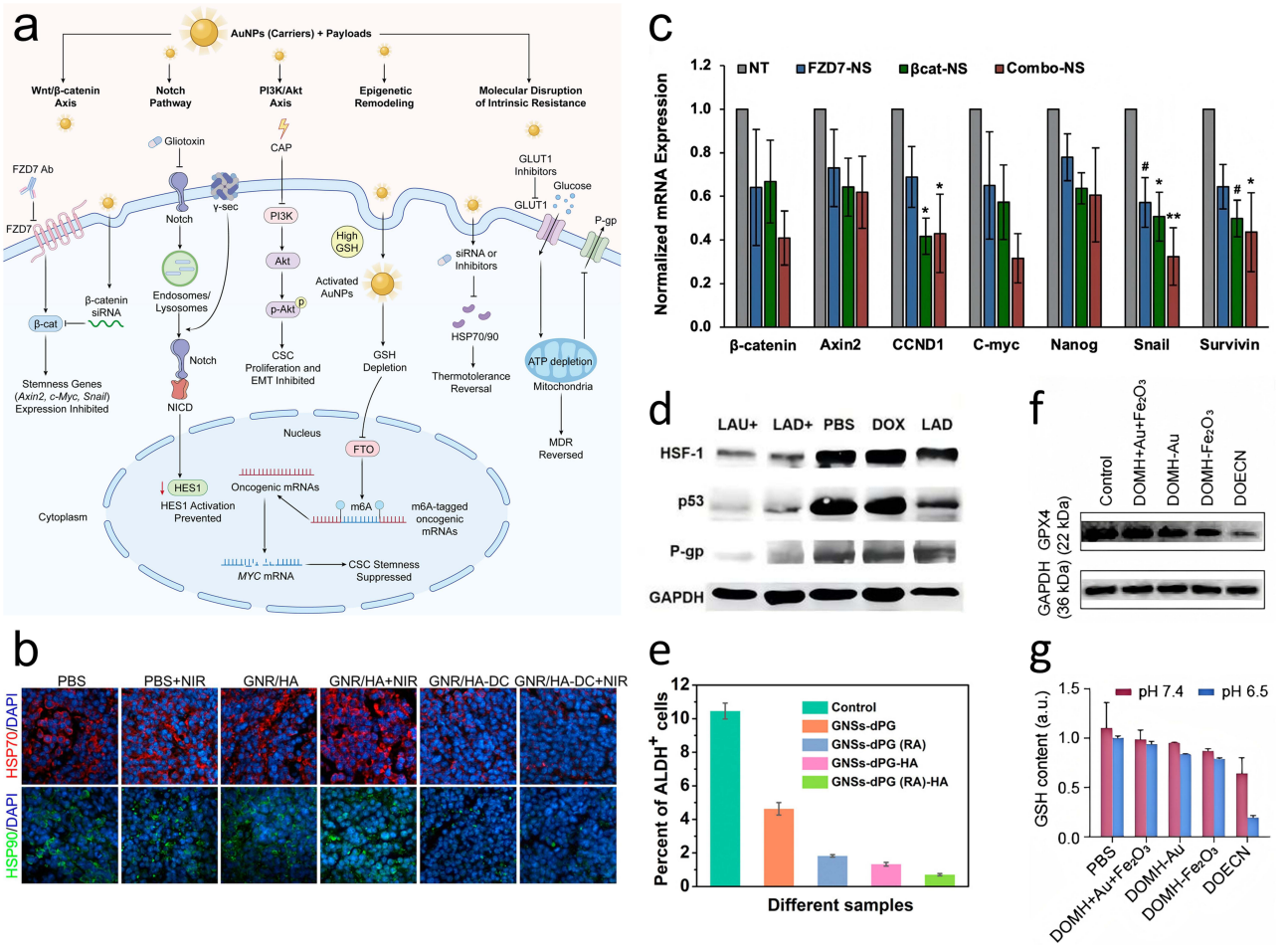

Figure 2 Molecular mechanisms of AuNP-mediated phenotypic reprogramming and metabolic modulation. This composite figure demonstrates specific biological interventions targeting CSC survival pathways. (**a**) Schematic illustration of the intracellular trafficking and multi-pathway targeting strategies of AuNPs, highlighting the simultaneous blockade of morphogenic signaling, epigenetic remodeling, and the molecular disruption of intrinsic resistance. (**b**) Chaperone suppression: Immunofluorescence images displaying the expression of HSP70 and HSP90 in tumor tissues following treatment, countering the heat shock response. (**c**) Wnt signaling inhibition: Representative RT-qPCR analysis showing the relative mRNA expression levels of β-catenin and downstream targets. (**d**) Resistance reversal: Western blot analysis confirming the suppression of P-glycoprotein (P-gp) expression. (**e**) Stemness reduction: Flow cytometric analysis of ALDH activity, where the reduction in the ALDH-positive subpopulation quantifies the efficacy of phenotypic differentiation strategies. (**f**) Redox modulation: Western blot analysis verifying the suppression of the anti-ferroptotic regulator GPX4. (**g**) Quantification of intracellular glutathione (GSH) levels, demonstrating the depletion of antioxidant capacity.
Notes: In panel (**a**), blunt-ended lines (⊥) indicate pathway blockade or inhibition. GAPDH was utilized as a loading control in all Western blot analyses. Quantitative data are presented as mean ± SD (n = 3). Statistical significance is denoted by * $p < 0.05$, ** $p < 0.01$, and # $p < 0.10$ versus the untreated (NT) group. Adapted with permission from the following sources: panel (**b**), Ref,[6] Copyright 2014 American Chemical Society; panel (**c**), Ref,[14] Copyright 2024 Wiley-VCH; panel (**d**), Ref,[53] Copyright 2020 Elsevier; panel (**e**), Ref,[48] Copyright 2021 American Chemical Society; panels (**f** and **g**), Ref,[58] Copyright 2025 American Association for the Advancement of Science.
Abbreviations: CAP, cold atmospheric plasma; FZD7, frizzled class receptor 7; NICD, Notch intracellular domain; GSH, glutathione; FTO, fat mass and obesity-associated protein; m^6A, N6-methyladenosine; GLUT1, glucose transporter 1; P-gp, P-glycoprotein.

Immunological Remodeling of the Tumor Niche

While bioenergetic and ferroptotic pathways achieve targeted cell death, remaining necrotic and apoptotic debris can form an immunosuppressive niche if not cleared. To prevent recurrence, treatment must shift from cytotoxicity to systematic niche remodeling. This stage aims to reverse the immune-silent CSC phenotype and convert the immunosuppressive TME into an immune-active state. Key steps include turning dying cells into in situ vaccines and normalizing stromal barriers.

Physical Triggering of Immunogenic Cell Death

Conventional thermal ablation uses temperatures above 50 °C, which non-specifically denature proteins and destroy potential tumor-associated antigens (TAAs). In contrast, effective systemic immunity requires mild photothermal heating (around 43–45 °C) that acts not just as a thermal source but as a physical trigger for ICD. Compared with differentiated

Table 1 Molecular Targets and Synergistic Mechanisms of AuNP-Mediated CSC Suppression

Therapeutic Dimension	Specific Molecular Target	AuNP-Based Strategy & Mechanism	Biological Outcome	References
Epigenetic Remodeling	FTO / m^6A Demethylases	GSH-bioimprinted nanoparticles deplete intracellular GSH to oxidize Fe^{2+} cofactors, enzymatically inactivating FTO/ALKBH5.	Increases m^6A methylation on *SNAI1* and *MYC* transcripts, driving RNA degradation and cellular differentiation.	Cao et al[13]
	HSP70 / P300 Complex	Quinacrine-gold hybrid nanoparticles inhibit HSP70 nuclear entry, deregulating the HSP70-P300 complex.	Reduces H3K14 acetylation, resulting in chromatin compaction and suppression of TGF-β.	Dash et al[39]
Signaling Blockade	Wnt / β-catenin	Combinational gold nanoshells co-deliver FZD7 antibody for receptor blockade and β-catenin siRNA for gene silencing.	Suppresses downstream Axin2 and c-Myc, mediating phenotypic locking via MET.	Dang et al[14]
	Notch / HIF-1α	Folic acid-functionalized gold nanoclusters deliver gliotoxin to disrupt the Notch-hypoxia axis.	Downregulates HES1 and Notch1, inhibiting secondary sphere formation.	Nambiar et al[42]
	Hedgehog (Gli1)	Spherical nucleic acids (SNAs) facilitate scavenger receptor-mediated uptake of siRNA to silence Gli1.	Downregulates ABCG2 transporters, sensitizing cells to chemotherapy.	Melamed et al[44]
Metabolic Subversion	Hexokinase 2 (HK2)	Mitochondria-targeted AuNPs deliver 3-bromopyruvate to the outer mitochondrial membrane.	Dissociates HK2 from VDAC, halting glycolytic flux and inducing apoptosis.	Marrache et al;[64] Pan et al[65]
	P-glycoprotein (*MDR1*)	AuNP-mediated mitochondrial disruption depletes the intracellular ATP pool required for efflux function.	Induces functional paralysis of ATP-dependent efflux pumps, enhancing drug retention.	Gaiser et al;[52] Liu et al[56]
Cell Death Execution	GPX4 / SLC7A11	Gold-based nanoreactors deplete GSH and amplify reactive oxygen species via Fenton-like chemistry.	Accumulates lipid peroxides, driving targeted cell death via GPX4 inactivation.	Zhang et al;[57] Jiao et al[58]
Thermotolerance Reversal	HSP90 / HSP70	Multifunctional gold nanoprobes induce glucose starvation or co-deliver pharmacological inhibitors such as ganetespib	Prevents stress-induced chaperone upregulation, sensitizing cells to mild photothermal therapy.	Fan et al;[67] Liu et al[68]

https://doi.org/10.2147/IJN.S606614

tumor cells, CSCs naturally evade immune surveillance by downregulating antigen-processing machinery and suppressing surface calreticulin (CRT). AuNP-mediated mild heat stress breaks this immune tolerance by spatiotemporally releasing damage-associated molecular patterns (DAMPs): surface CRT acts as an "eat-me" signal; extracellular ATP acts as a "find-me" chemotactic cue; and secreted HMGB1 promotes dendritic cell (DC) maturation.

Recent advances combine this mild thermal stress with molecular adjuvants to strengthen immune responses. For example, mesoporous silica-coated gold nanorods modified with HA co-deliver the TLR7 agonist R837. Under NIR irradiation, the construct produces mild hyperthermia to induce ICD, while released R837 boosts DC maturation and reverses immunosuppression in triple-negative breast cancer.[75] This strategy is further improved using biological carriers such as attenuated *Salmonella* coated with gold nanoparticles. These biohybrids actively penetrate hypoxic regions and, after photothermal activation, release tumor antigens together with GM-CSF to recruit DCs into the tumor core and establish long-term immune memory.[76]

In addition to thermal triggers, AuNPs can induce ICD through chemodynamic and pyroptotic pathways. DNA origami-based nanoreactors, which spatially organize AuNPs and iron oxide clusters, amplify Fenton-type reactions. The resulting oxidative stress cascade acts as a strong ICD inducer that converts the TME into an immunogenic niche.[58] Furthermore, disrupting ion balance provides a new immune activation route. Dual-pathway nanoreactors based on Au–CuSe@ZIF-8 structures trigger pyroptosis—a highly inflammatory form of cell death—through zinc ion overload and ROS accumulation. This lytic cell death releases large amounts of DAMPs and inflammatory cytokines, strongly activating adaptive immunity.

Notably, antigen release alone is often insufficient if antigens are degraded before processing. To solve this problem, antigen-trapping systems have been developed using polyphenol-modified gold nanorods. Galloyl groups on these nanorods form strong hydrogen bonds with proteins released during photothermal lysis, trapping TAAs on the nanoparticle surface as molecular anchors. This nanovaccine complex improves antigen uptake by antigen-presenting cells and promotes lymph node migration, greatly increasing cytotoxic T-cell infiltration into tumor parenchyma.[77] The biological cascade from local nanotherapeutic stress to strong ICD and systemic immune remodeling is illustrated in Figure 3.

Normalization of Stromal and Hypoxic Barriers

While ICD induction recruits effector T cells to the tumor periphery, their infiltration and survival in the solid tumor core are blocked by a dual-layer defense system: the physical desmoplastic barrier and chemical hypoxic stress. The physical barrier, formed by cancer-associated fibroblasts (CAFs) and dense extracellular matrix (ECM), generates high interstitial fluid pressure that mechanically excludes drugs and immune cells.[80]

Recent studies using iron oxide–gold hybrid nanoflowers show that mild photothermal therapy can selectively eliminate CAFs. This depletion reduces collagen deposition and normalizes tumor stiffness, thereby restoring vascular perfusion.[81] Importantly, AuNPs also mechanically disrupt focal adhesion complexes in stromal cells, further loosening the structural stability of the niche.[82] A key concern is that such matrix softening might accidentally promote autophagy-related survival or metastatic escape.[83] However, this risk is effectively controlled by the upstream phenotypic locking (MET) strategy described earlier: by fixing CSCs in a non-motile state, the approach creates a permissive environment for T-cell entry while maintaining a restrictive environment for tumor cell dissemination.

Alongside physical barrier breakdown, the immunosuppressive chemical environment of the niche must be neutralized to support aerobic immune effector functions. The hypoxic tumor core acts as a protective metabolic niche in which HIF-1α stabilizes stemness and suppresses T-cell activity. To address this issue, gold nanostructures modified with manganese dioxide (MnO_2) shells or nitric oxide (NO) donors have been developed to actively re-oxygenate the microenvironment. The reaction between MnO_2 and endogenous H_2O_2 produces oxygen in situ and consumes protons, relieving both hypoxia and acidosis.[68] At the same time, NO-mediated vasodilation improves blood perfusion, creating a normoxic window that acts synergistically with physical stromal relaxation to fully disrupt the defensive CSC niche.[59]

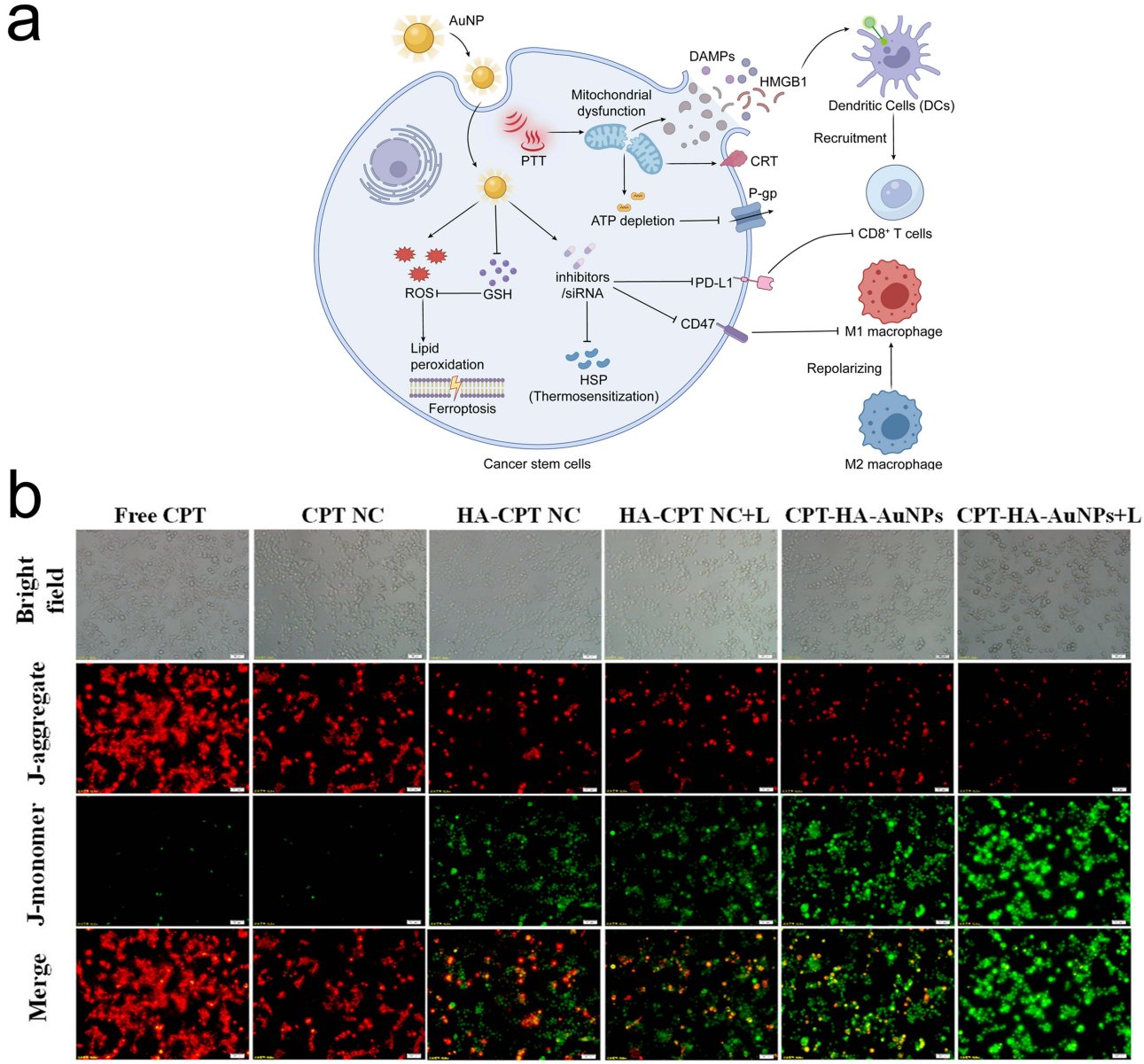

Figure 3 Evaluation of photothermal-induced cell death and immune microenvironment remodeling. Analysis of the biological cascades initiated by mild photothermal stimulation. (**a**) Schematic overview of AuNP-mediated biological cascades, highlighting the induction of ferroptosis via redox disruption (GSH depletion and ROS amplification), alongside comprehensive immune microenvironment remodeling through immunogenic cell death (ICD) and the intracellular silencing of immune checkpoints (CD47 and PD-L1). (**b**) Organelle dysfunction: JC-1 staining assays indicating the loss of mitochondrial membrane potential ($\Delta\Psi_m$). (**c**) Lipid peroxidation: Confocal imaging using BODIPY C11 showing the accumulation of lipid peroxides, indicating the induction of ferroptosis. (**d**) In vivo thermotolerance inhibition: Immunohistochemical (IHC) staining of tumor sections showing decreased HSP72 expression in the targeted treatment group, confirming the sensitization of tumor cells to mild hyperthermia. (**e–g**) Immunogenic cell death (ICD) and immune infiltration: (**e**) Confocal imaging of calreticulin (CRT) exposure on the cell surface serving as an "eat me" signal. (**f**) Macrophage repolarization: Flow cytometric analysis of tumor-associated macrophages, evaluating the expression of CD86 (M1-like) and MMR (M2-like) markers to demonstrate the phenotypic shift from M2 to M1 following treatment with cetuximab-conjugated AuNRs (CTX-AuNR) plus NIR irradiation. (**g**) Flow cytometric analysis demonstrating downstream immune activation and cytotoxic T lymphocyte infiltration in tumor tissues.

Notes: In panel (**a**), blunt-ended lines (⊥) indicate pathway blockade or gene silencing. In panel (**d**), cell nuclei are counterstained blue with hematoxylin, and HSP72 expression is indicated by the brown DAB signal. Quantitative data are represented as mean ± SD (n = 3). Statistical significance is denoted by *** $p < 0.001$. The scale bars are 50 μm in panels (**b**) and (**d**), and 20 μm in panel (**e**). Adapted with permission from the following sources: panel (**b**), Ref,[54] Copyright 2022 American Chemical Society; panel (**c**),[78], licensed under CC BY; panel (**d**), Ref,[9] Copyright 2016 American Chemical Society; panel (**e**), Ref,[11] Copyright 2016 American Chemical Society; panel (**f**), Ref,[79] Copyright 2025 American Chemical Society; panel (**g**), Ref,[11] Copyright 2016 American Association for the Advancement of Science.

Abbreviations: AuNP, gold nanoparticle; CSC, cancer stem cell; PTT, photothermal therapy; HSP, heat shock protein; GSH, glutathione; ROS, reactive oxygen species; CRT, calreticulin; HMGB1, high mobility group box 1; DAMPs, damage-associated molecular patterns; DCs, dendritic cells; PD-L1, programmed death-ligand 1.

https://doi.org/10.2147/IJN.S606614

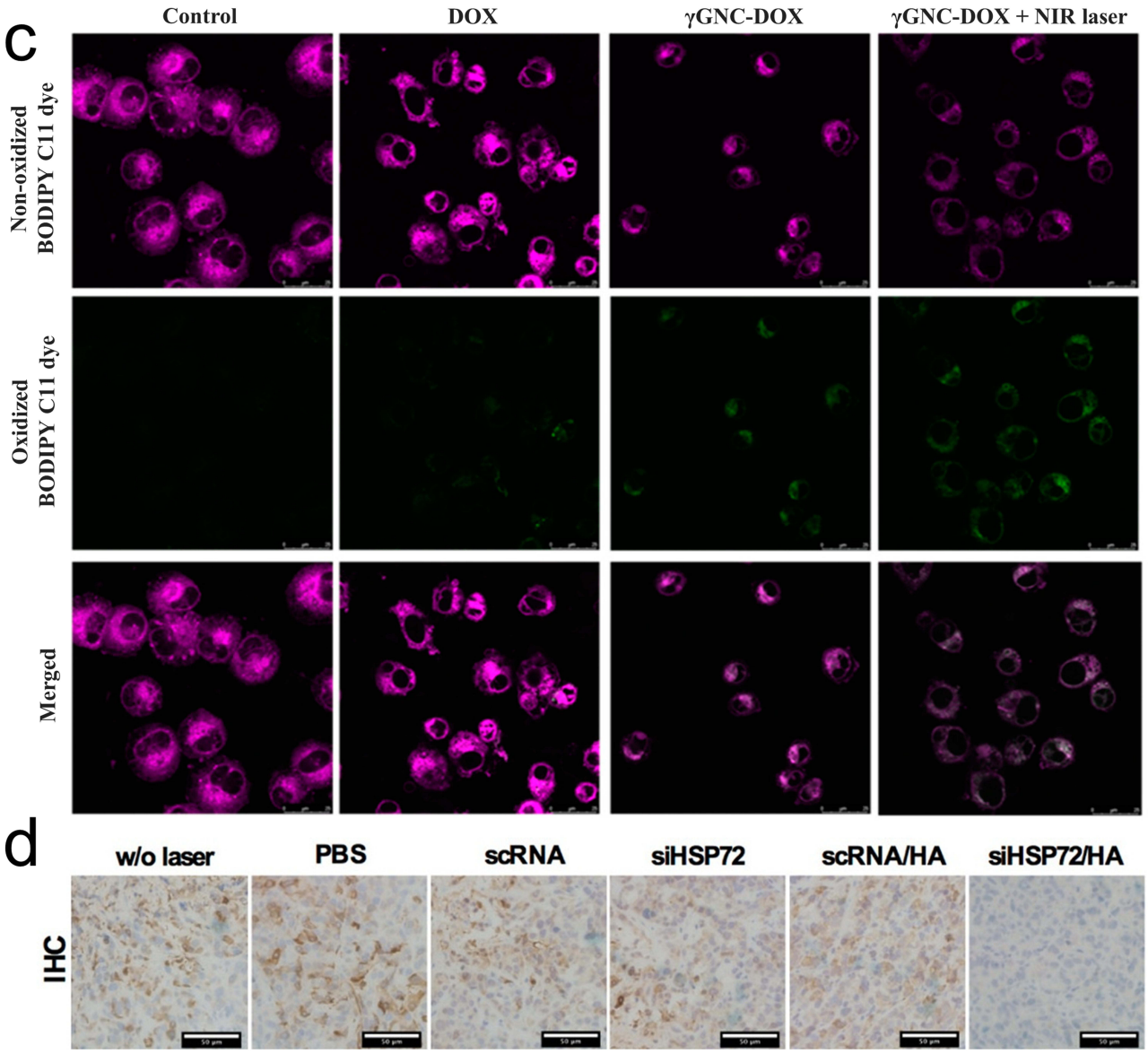

Figure 3 Continued.

Dismantling Immune Checkpoint Tolerance

After physical barriers are removed and the chemical microenvironment is normalized, immune checkpoint evasion—the last line of CSC defense—must be blocked to enable effector cell function. Unlike bulk tumor cells, CSCs specifically upregulate surface ligands to inhibit infiltrating immune cells: CD47 serves as a key anti-phagocytic signal against macrophage surveillance, while programmed death-ligand 1 (PD-L1) strongly inhibits cytotoxic T-cell activity.

To overcome the innate immune barrier, engineered bacterial biohybrids (eVNP@AuNFs) have been created, combining the hypoxia-targeting ability of attenuated *Salmonella* with the photothermal properties of gold nanoflowers. This system uses bacteria to deliver short hairpin RNA (shRNA) plasmids that downregulate CD47, while the gold component simultaneously inhibits HSP90 through mild hyperthermia. Mild thermal stress in the tumor core, combined with genetic silencing of the CD47–SIRPα axis, reactivates macrophage phagocytosis and triggers a systemic antigen-specific immune response.[11] Specific targeting strategies such as cetuximab-conjugated gold nanorods (CTX-AuNR) can synergize with mild photothermal therapy to directly reprogram tumor-associated macrophages from a pro-tumor M2 phenotype toward an anti-tumor M1 state, establishing a robust anti-tumor immune microenvironment.[79]

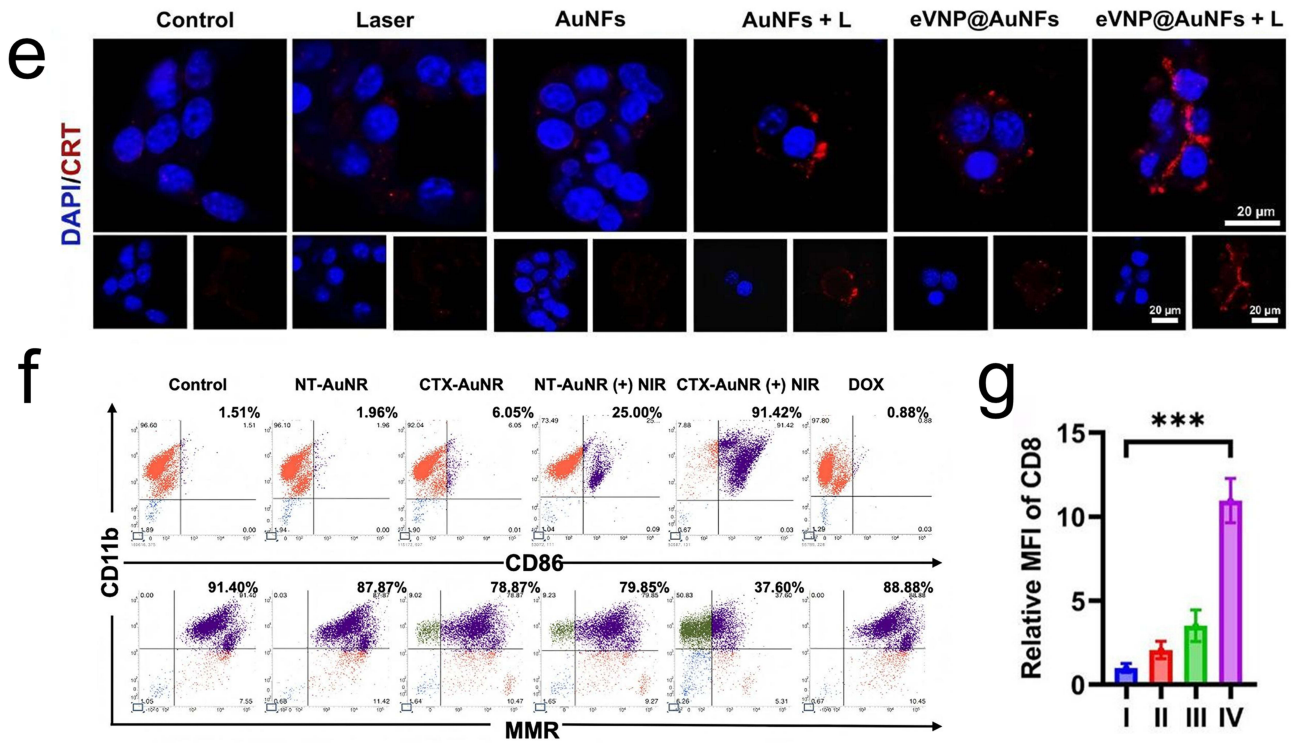

Figure 3 continued.

To enhance the adaptive immune response, the PD-1/PD-L1 pathway is targeted in parallel. Surface-engineered gold nanorods modified with layer-by-layer polyelectrolytes are designed to deliver siRNA targeting PD-L1. This construct specifically acts on post-EMT CSCs, which often show elevated PD-L1 expression. Downregulation of PD-L1 relieves inhibitory signaling on tumor-infiltrating lymphocytes, ensuring that cytotoxic cells recruited into the normalized niche remain functionally active. This sequential integration of physical access, chemical re-oxygenation and checkpoint inhibition achieves comprehensive suppression of the resistant CSC population.[84]

Discussion and Future Perspectives

The shift from regulating molecular pathways to achieving targeted cell death marks a key paradigm change in CSC-targeted nanomedicine. However, translating these complex laboratory designs into clinical practice remains limited by the high adaptive plasticity of CSCs and the lack of real-time treatment monitoring. The future of gold-based therapy does not depend solely on stronger cytotoxicity, but on building an adaptive closed-loop system that responds to the constantly changing tumor microenvironment.

The Paradox of Static Thermal Ablation

Moving from targeted niche remodeling to clinical use reveals major translational barriers. Because of strong intratumoral heterogeneity and irregular vascularization, achieving uniform lethal temperatures during conventional PTT is technically difficult. Clinical studies of early silica-core gold nanoshells show that using static thermal dosimetry often leads to inconsistent therapeutic effects. Instead of producing uniform ablation, this static strategy frequently exposes peripheral tumor regions to sublethal thermal stress.

Sublethal heating actively promotes an adaptive survival phenotype in residual tumor cells. Transcriptomic and cellular studies show that temperatures near 48 °C induce rapid necrosis, while mild thermal stress around 43 °C triggers a protective autophagic response. This autophagy recycles damaged organelles and helps maintain dormancy in surviving cells. As a result, insufficient thermal dosing acts as a selective pressure that may enrich thermotolerant CSCs. This

https://doi.org/10.2147/IJN.S606614

resistance is further strengthened by the rapid upregulation of HSPs, which stabilize denatured proteins and suppress apoptotic pathways.[83,85]

To overcome these intrinsic biological defenses, next-generation AuNPs are strategically designed to combine physical heating with active molecular intervention. Preclinical studies confirm that depleting specific chaperones via targeted siRNA delivery or metabolic inhibitors greatly reduces thermal resistance. This combined approach allows even mild hyperthermia to effectively suppress malignant cells without relying on extreme temperatures. Therefore, moving AuNP platforms toward clinical translation requires a shift from static physical interventions to dynamic systems that integrate real-time biological feedback to verify treatment efficacy. Table 2 summarizes these translational obstacles and corresponding mechanism-based solutions.[6,9]

Establishing the Theranostic Closed-Loop

To overcome the limitations of static dosimetry, next-generation gold nanoplatforms have developed into theranostic closed-loop systems. In this design, the inherent plasmonic properties of gold are used simultaneously to process biological signals and control therapeutic outputs. Compared with fluorescence, surface-enhanced Raman scattering (SERS) provides molecular fingerprint specificity that can identify unique metabolic signatures of resistant CSCs in situ. This supports adaptive nanotherapy, in which treatment intensity is adjusted in real time based on biological responses.

It is important to clarify that this closed-loop system does not yet operate fully autonomously. Instead, it mainly depends on external guidance, using macroscopic optical signals including SERS and photoacoustic (PA) imaging to direct precise manual laser triggering.

The main function of this loop is real-time evaluation of resistance and confirmation of complete cell elimination. Advanced gold substrates enable molecular mapping of the CSC niche by visualizing the accumulation of antioxidant metabolites such as hypotaurine,[10] and resistance-related polysulfides.[86] Once activated, organelle-targeted nanoprobes monitor dynamic molecular stress responses. Changes over time in specific SERS peaks related to tryptophan and phenylalanine serve as quantitative markers for protein denaturation and nuclear fragmentation.[87] This provides direct spectral evidence of irreversible apoptosis, ensuring that thermal doses are sufficient to prevent the survival of thermotolerant cells.

Table 2 Bridging the Translational Gap: Mechanistic Shortcomings of Clinical AuNP Platforms and Next-Generation Solutions

Clinical/Pre-clinical Platform	Mechanistic Limitation/ Failure Mode	Next-Generation Bio-Nano Solution	References
AuroLase® Therapy (Silica-Core Au Nanoshells)	Reliance on static thermal dosimetry often results in sublethal hyperthermia (~43 °C) at tumor margins. This stress triggers HSP upregulation and autophagy-mediated survival in CSCs, rather than necrosis.	Integration of real-time thermal monitoring (PAI/SERS) with metabolic inhibitors such as 3-BP and ganetespib to disable the heat-shock response prior to ablation.	Zhao et al;[85] Ghafarkhani et al;[83] Wang et al[9]
CYT-6091 (AuNP-TNFα)	Dependence on passive accumulation leads to rapid sequestration by the mononuclear phagocyte system and insufficient intratumoral dose, causing systemic toxicity.	Deployment of biomimetic erythrocyte or platelet membrane coatings to evade clearance, or utilizing mesenchymal stem cells (MSCs) and macrophages as cellular carriers to breach physiological barriers.	Alle et al;[16] Hu et al;[26] Rosu et al[30]
First-generation targeted AuNPs with single-ligand modification such as anti-EGFR	Formation of the protein corona in vivo masks surface ligands, rendering targeting ineffective. Furthermore, single-receptor targeting suffers from off-target toxicity on normal stem cells.	Implementation of dual-input systems integrating CD44 binding with acidic pH or metabolic activation, or stimuli-responsive sheddable shells that expose the targeting moiety strictly within the tumor microenvironment.	Nel et al;[12] Zhang et al;[38] Li et al[37]
Conventional Chemo-AuNPs (Passive Drug Loading)	Passive drug release is countered by upregulated ABC transporters (eg, P-gp) in CSCs, which actively efflux the payload, maintaining sub-lethal intracellular concentrations.	Use of mitochondria-targeted AuNPs to physically disrupt the electron transport chain and deplete ATP, thereby cutting off the energy supply required for P-gp efflux function.	Chen et al;[66] Gaiser et al[52]
Standard Radiosensitization (High-Z AuNPs alone)	While AuNPs enhance local radiation dose via the Auger effect, radioresistant CSCs rapidly repair DNA double-strand breaks via upregulated repair pathways, leading to tumor recurrence.	Engineering AuNPs as peroxidase mimics or Fenton-like catalysts to amplify intracellular reactive oxygen species (ROS), overwhelming the DNA repair machinery with targeted oxidative stress.	Atkinson et al;[5] Jiao et al[58]

Table 3 Integrated Theranostic Strategies for Niche Remodeling and Real-Time Surveillance

Target Dimension	AuNP-Mediated Strategy	Monitoring Modality	Quantitative Readout/Metric	References
Physical Stroma	Photothermal depletion of CAFs coordinated with MET induction to restrict metastasis.	Photoacoustic elastography	Reduction in Young's modulus; Decreased collagen I/III ratio.	Nicolás-Boluda et al;[81] Mulens-Arias et al[82]
Chemical Niche	MnO_2-catalyzed O_2 generation and NO-mediated vasodilation to alleviate hypoxia.	Oxygen-enhanced photoacoustic imaging	Increase in oxy-hemoglobin (HbO_2) signal intensity; pH normalization.	Liu et al;[68] Wang et al[59]
Metabolic Adaptation	Label-free spectral detection of resistance-associated antioxidant metabolites.	Surface-enhanced Raman scattering (SERS)	SERS peaks for polysulfides (480 cm^{-1}) and hypotaurine.	Shiota et al;[10] Honda et al[86]
Cellular Fate	Real-time monitoring of intracellular protein denaturation and nuclear fragmentation.	Organelle-targeted SERS	Evolution of phenylalanine and tryptophan SERS peaks.	Qi et al;[87] Hu et al[88]
Thermal Dosimetry	Converting thermal expansion into volumetric maps to identify sublethal regions.	Macroscopic photoacoustic imaging	3D temperature distribution mapping (ΔT) in deep tissue.	Hu et al;[88] Joseph et al[35]
Immune Landscape	Trapping tumor-associated antigens combined with CD47/PD-L1 silencing.	Immuno-SERS and fluorescence imaging	Ratio of $CD86^+$/ $CD206^+$ macrophage expression; IFN-γ levels.	Ye et al;[77] Sun et al;[11] Arellano et al[84]

However, the limited tissue penetration of SERS requires combined use with deep-tissue imaging methods. The strong near-infrared absorption of gold allows PA imaging to continuously monitor macroscopic temperature distributions and identify deep regions with insufficient heat diffusion, while SERS characterizes subcellular metabolic differences.

This macro-micro integration is achieved through advanced nanostructure design, such as double-walled gold nanocages[88] or manganese-doped hybrid systems.[35] These structures act as both SERS sensors and photothermal converters. This comprehensive integration, which links metabolic detection and macroscopic monitoring to adaptive treatment, is summarized in Table 3. The working mechanism of these advanced functions is shown in Figure 4, providing a structural basis for solving manufacturing challenges in clinical translation.

Translational Bottlenecks and Manufacturing Realities

Although closed-loop theranostics and biomimetic surface engineering provide a reasonable theoretical framework for overcoming therapeutic resistance, translating these advanced gold nanoplatforms into clinical use requires addressing key pharmacokinetic and manufacturing limitations. Although preliminary proof-of-concept models demonstrate short-term histological safety and biocompatibility across major organs,[89] the main biological challenge remains the long-term accumulation and unclear safety of metal nanoparticles in vivo.

Even with surface coatings, particles that leave the tumor or degrade over time can be marked by opsonization and trapped by RES. Biodistribution studies consistently show that intravenously injected gold nanostructures, especially those larger than the renal filtration limit, mainly accumulate in liver and spleen macrophages. These particles remain in these organs for long periods without significant degradation.

Long-term tissue retention raises clear safety concerns, including excess liver load and potential immune interference. These issues challenge the clinical feasibility of using non-biodegradable noble metals for repeated treatment.[90,91]

In addition, the clinical translation of biomimetic modification, especially coatings from erythrocytes or platelets, is currently limited by large-scale production challenges. Although these biological membranes show excellent immune evasion and tumor-homing ability in highly controlled laboratory settings, scaled production leads to significant batch-to-batch differences.

The physical processes used for membrane isolation and nanoparticle coating, including mechanical extrusion or ultrasonication, tend to impair the fine structure of extracellular vesicles. Such intense physical treatment may lead to the loss of key transmembrane proteins, disordered protein orientation, and altered lipid component ratios. As a result, the final products exhibit unstable physicochemical properties, resulting in unpredictable pharmacokinetic profiles and inconsistent therapeutic efficacy during large-scale production.[92–94]

Beyond manufacturing variability, the regulatory pathway for biomimetic gold systems represents another major hurdle for clinical translation. These advanced platforms integrate synthetic inorganic metal cores and biologically derived

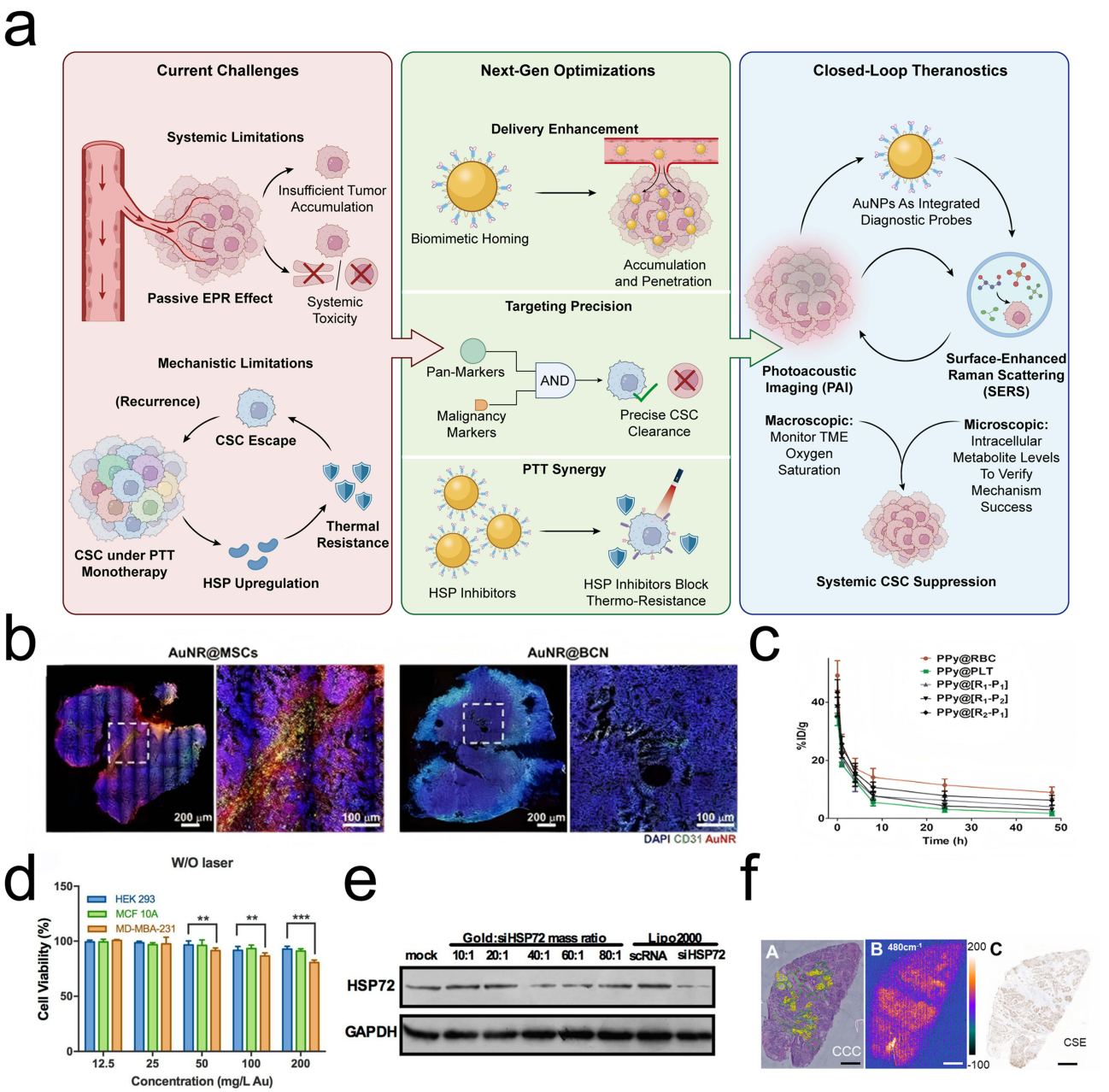

Figure 4 Optimization of delivery kinetics and real-time theranostic monitoring. Characterization of the delivery efficiency, targeting specificity, and feedback capabilities of the AuNP platform. (**a**) Schematic overview of the next-generation theranostic closed-loop system, illustrating the progression from overcoming systemic and mechanistic limitations to achieving precise CSC suppression. The framework highlights biomimetic camouflage and AND-gated logic for targeted delivery, integrated with a macroscopic-microscopic surveillance loop using photoacoustic imaging (PAI) and surface-enhanced Raman scattering (SERS) for real-time therapeutic feedback. (**b**) Delivery efficiency: Fluorescence imaging of tumor sections showing the deep penetration of MSC-mediated AuNP carriers compared to passive controls. (**c**) Pharmacokinetic profiles demonstrating the prolonged blood circulation half-life conferred by biomimetic erythrocyte membrane coatings compared to bare nanoparticles. (**d**) Logic-gated selectivity: Cell viability assays illustrate the precision of the AND-gate targeting strategy. The striking contrast in therapeutic efficacy between dual-positive target cells CD44+/$HSP72_{high}$ (target) versus CD44+/$HSP72_{low}$ (non-target) confirms that this dual-recognition system successfully mitigates off-target toxicity. (**e**) Gene silencing efficiency: Western blot analysis confirming the knockdown efficiency of siHSP72 delivered by the gold nanoplatform. (**f**) SERS metabolic mapping: Surface-enhanced Raman scattering (SERS) spectral imaging of tumor tissues. The heatmaps visualize the spatial distribution of polysulfides at 480 cm^{-1}, providing label-free metabolic feedback for therapeutic assessment. (**g**) Photoacoustic imaging: In vivo mapping of deep tumor architecture and oxygenation saturation (SO_2/HbO_2), demonstrating real-time surveillance of deep tumor regions. (**h**) In vivo temperature monitoring: Real-time thermal mapping during near-infrared laser actuation. (**i**) Quantitative analysis of photothermal conversion efficiency across different treatment groups. (**j**) Biodistribution analysis charting nanoplatform accumulation across major organs over time. (**k**) Histological evaluation of major organs indicating the systemic safety and biocompatibility of the engineered nanoplatforms.

Notes: In panel (**a**), green ticks and red crosses indicate successful therapeutic optimizations and specific limitations or cleared cells, respectively. Quantitative assay results are expressed as mean ± SD (n = 3 for Western blotting, n = 5 for cell viability). Statistical significance is indicated with asterisks (** $p < 0.01$, *** $p < 0.001$). Dashed boxes and circles highlight selected regions of interest in the respective panels. The scale bars are 50 μm in panel (**b**); 1 mm in panel (**f**); 2 mm in panel (**g**); and 250 μm in panel (**k**). Adapted with permission from the following sources: panels (**b, h, i** and **j**), Ref,[31] licensed under CC BY; panel (**c**), Ref,[29] Copyright 2018 Royal Society of Chemistry; panels (**d** and **e**), Ref,[9] Copyright 2016 American Chemical Society; panel (**f**), Ref,[86] Copyright 2021 Elsevier; panel (**g**), Ref,[68] Copyright 2023 American Chemical Society; panel (**k**), Ref,[89] licensed under CC BY.

Abbreviations: EPR, enhanced permeability and retention; AuNPs, gold nanoparticles; CSC, cancer stem cell; PTT, photothermal therapy; HSP, heat shock protein; SERS, surface-enhanced Raman scattering; PAI, photoacoustic imaging; TME, tumor microenvironment.

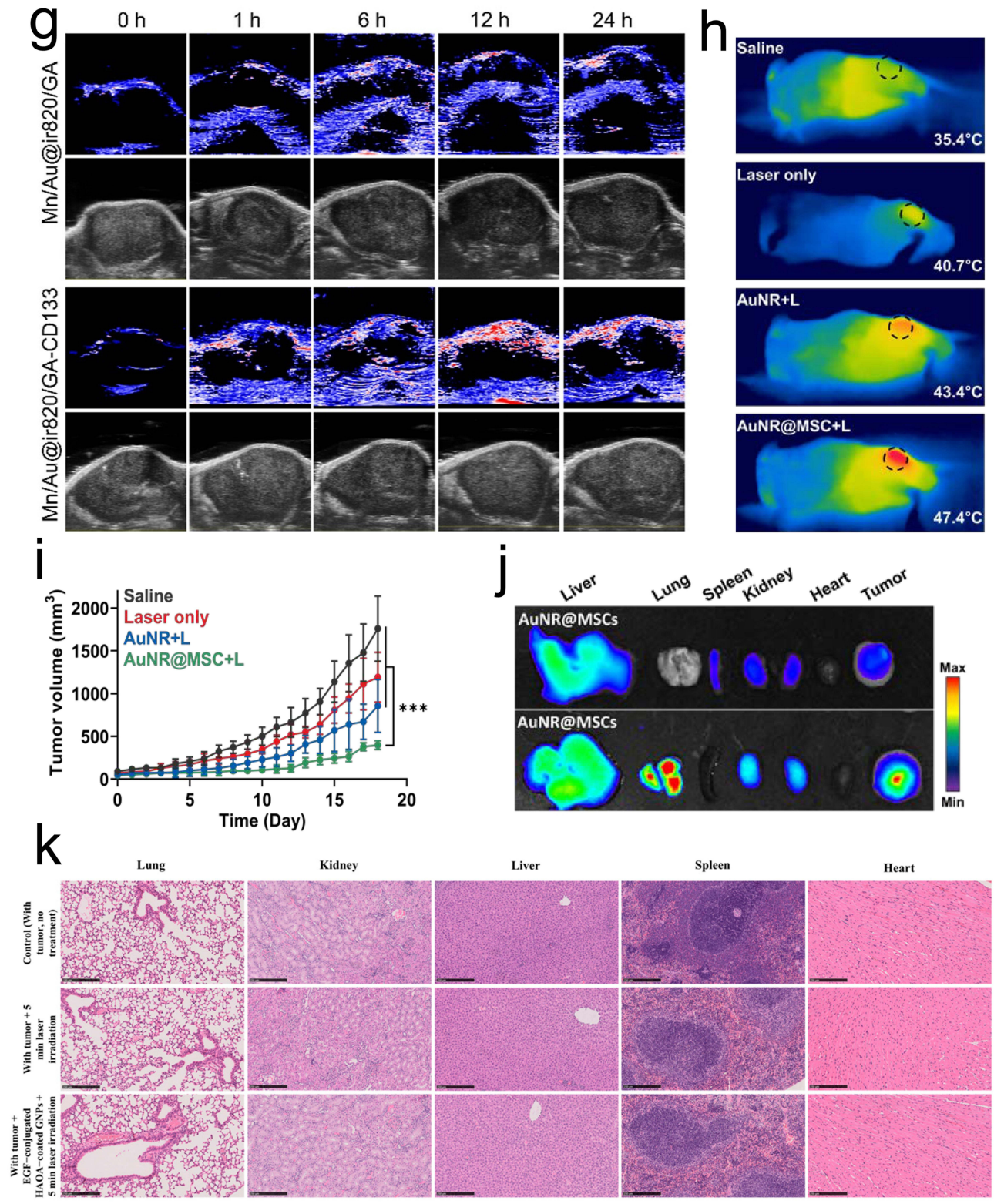

Figure 4 Continued.

functional membranes, leading to considerable regulatory complexity. Regulatory agencies struggle to classify these hybrid constructs, since they display combined features of chemical drugs, biological products, and medical devices simultaneously.

https://doi.org/10.2147/IJN.S606614

They are therefore typically assessed under the strict and overlapping evaluation standards applied to complex combination products. This classification significantly raises the demands for quality control, including rigorous sterility validation of raw materials, comprehensive immunogenicity testing, and full adherence to Good Manufacturing Practice (GMP) guidelines.[92,95] Ultimately, translating these sophisticated adaptive nanomedicines into clinically usable formulations requires closing the gap between small-scale laboratory synthesis and standardized, scalable industrial manufacturing.

Conclusion

The effective suppression of cancer stem cells requires a fundamental departure from non-specific cytotoxicity to precision biological engineering. This review has delineated a comprehensive therapeutic strategy that evolves from the logic-gated infiltration of the tumor niche to the targeted phenotypic locking of plastic populations, followed by their metabolic and organelle-specific disruption. By subsequently normalizing the desmoplastic stroma and dismantling immune checkpoints, this multi-modal approach systematically dismantles the protective microenvironmental niches of the residual disease. Ultimately, the integration of SERS-guided feedback loops and macroscopic photoacoustic surveillance transforms the gold nanoparticle from a static photothermal agent into a dynamic, adaptive computational node. Future clinical translation will depend not on the development of materials with higher photothermal conversion efficiencies, but on the engineering of responsive systems capable of interpreting the metabolic heterogeneity of the tumor and responding with systemic safety and adaptive, therapeutic precision, thereby bridging the critical gap between nanoscale design and standardized clinical translation.

Data Sharing Statement

No primary research results, software or code have been included and no new data were generated or analysed as part of this review.

Author Contribution

All authors made a significant contribution to the work reported, whether that is in the conception, study design, execution, acquisition of data, analysis and interpretation, or in all these areas; took part in drafting, revising or critically reviewing the article; gave final approval of the version to be published; have agreed on the journal to which the article has been submitted; and agree to be accountable for all aspects of the work.

Funding

This project was supported by Basic Research Program of Shenzhen Innovation Council (JCYJ20250604183723030); Guangdong Provincial Medical Science and Technology Research Fund (A2024488), Shenzhen Clinical Medical Research Center for Oral Diseases (Grant No. 20210617170745001-SCRC202201001), the Sanming Project of Medicine in Shenzhen (SZSM202111012, Oral and Maxillofacial Surgery Team, Professor Yu Guangyan, Peking University Hospital of Stomatology), and Shenzhen Fund for Guangdong Provincial High-level Clinical Key Specialties (SZGSP008).

Disclosure

The authors declare that they have no competing interests.

References

1. Clara JA, Monge C, Yang Y, Takebe N. Targeting signalling pathways and the immune microenvironment of cancer stem cells - a clinical update. *Nat Rev Clin Oncol*. 2020;17(4):204–232. doi:10.1038/s41571-019-0293-2
2. Shibue T, Weinberg RA. EMT, CSCs, and drug resistance: the mechanistic link and clinical implications. *Nat Rev Clin Oncol*. 2017;14(10):611–629. doi:10.1038/nrclinonc.2017.44
3. Xiong X, Arvizo RR, Saha S, et al. Sensitization of ovarian cancer cells to cisplatin by gold nanoparticles. *Oncotarget*. 2014;5(15):6453–6465. doi:10.18632/oncotarget.2203

4. Abbasian M, Baharlouei A, Arab-Bafrani Z, Lightfoot DA. Combination of gold nanoparticles with low-LET irradiation: an approach to enhance DNA DSB induction in HT29 colorectal cancer stem-like cells. *J Cancer Res Clin Oncol*. 2019;145(1):97–107. doi:10.1007/s00432-018-2769-3
5. Atkinson RL, Zhang M, Diagaradjane P, et al. Thermal enhancement with optically activated gold nanoshells sensitizes breast cancer stem cells to radiation therapy. *Sci Transl Med*. 2010;2(55):55ra79. doi:10.1126/scitranslmed.3001447
6. Chen WH, Luo GF, Lei Q, et al. Overcoming the heat endurance of tumor cells by interfering with the anaerobic glycolysis metabolism for improved photothermal therapy. *Acs Nano*. 2017;11(2):1419–1431. doi:10.1021/acsnano.6b06658
7. Karakocak BB, Liang J, Biswas P, Ravi N. Hyaluronate coating enhances the delivery and biocompatibility of gold nanoparticles. *Carbohydr Polym*. 2018;186:243–251. doi:10.1016/j.carbpol.2018.01.046
8. Young JL, Hua X, Somsel H, Reichart F, Kessler H, Spatz JP. Integrin subtypes and nanoscale ligand presentation influence drug sensitivity in cancer cells. *Nano Lett Feb*. 2020;20(2):1183–1191. doi:10.1021/acs.nanolett.9b04607
9. Wang S, Tian Y, Tian W, et al. Selectively sensitizing malignant cells to photothermal therapy using a CD44-targeting heat shock protein 72 depletion nanosystem. *ACS Nano*. 2016;10(9):8578–8590. doi:10.1021/acsnano.6b03874
10. Shiota M, Naya M, Yamamoto T, et al. Gold-nanofève surface-enhanced Raman spectroscopy visualizes hypotaurine as a robust anti-oxidant consumed in cancer survival. *Nat Commun*. 2018;9(1):1561. doi:10.1038/s41467-018-03899-1
11. Sun T, Wang MM, Zhang L, et al. Engineered bacterial biohybrid-mediated CD47-SIRPα blockade and HSP90 inhibition for enhanced immuno-photothermal therapy. *ACS Appl Mater Interf*. 2025;17(20):29183–29197. doi:10.1021/acsami.5c01645
12. Nel AE, Madler L, Velegol D, et al. Understanding biophysicochemical interactions at the nano-bio interface. *Nat Mater*. 2009;8(7):543–557. doi:10.1038/nmat2442
13. Cao K, Du Y, Bao X, et al. Glutathione-bioimprinted nanoparticles targeting of n6-methyladenosine fto demethylase as a strategy against leukemic stem cells. *Small*. 2022;18(13):e2106558. doi:10.1002/smll.202106558
14. Dang MN, Suri S, Li KJ, et al. Antibody and siRNA nanocarriers to suppress wnt signaling, tumor growth, and lung metastasis in triple-negative breast cancer. *Adv Therapeutics*. 2024;7(6). doi:10.1002/adtp.202300426
15. Li NN, Cheng JJ, Zhang Y, et al. A chemophotothermal and targeting multifunctional nanoprobe with a tumor-diagnosing ability. *Nano Res*. 2018;11(8):4333–4347. doi:10.1007/s12274-018-2021-0
16. Alle M, Sharma G, Lee SH, Kim JC. Next-generation engineered nanogold for multimodal cancer therapy and imaging: a clinical perspectives. Review. *J Nanobiotechnol*. 2022;20(1):222. doi:10.1186/s12951-022-01402-z
17. Li JC, Chen Y, Yang YJ, Kawazoe N, Chen GP. Sub-10 nm gold nanoparticles promote adipogenesis and inhibit osteogenesis of mesenchymal stem cells. *J Mater Chemistr B*. 2017;5(7):1353–1362. doi:10.1039/c6tb03276a
18. Jaiswal N, Mahata N, Chanda N. Nanogold-albumin conjugates: transformative approaches for next-generation cancer therapy and diagnostics. Review. *Nanoscale*. 2025;17(18):11191–11220. doi:10.1039/d4nr05279j
19. Maghsoudian S, Motasadizadeh H, Farhadnejad H, et al. Targeted pH- and redox-responsive AuS/micelles with low CMC for highly efficient sonodynamic therapy of metastatic breast cancer. *Biomater Adv*. 2024;158:213771. doi:10.1016/j.bioadv.2024.213771
20. Shamsian A, Sepand MR, Javaheri Kachousangi M, et al. Targeting tumorigenicity of breast cancer stem cells using SAHA/Wnt-b catenin antagonist loaded onto protein corona of gold nanoparticles. *Int J Nanomed*. 2020;15:4063–4078. doi:10.2147/ijn.S234636
21. Salvati A, Pitek AS, Monopoli MP, et al. Transferrin-functionalized nanoparticles lose their targeting capabilities when a biomolecule Corona adsorbs on the surface. *Nat Nanotechnol*. 2013;8(2):137–143. doi:10.1038/nnano.2012.237
22. Wang Z, Chen Z, Liu Z, et al. A multi-stimuli responsive gold nanocage-hyaluronic platform for targeted photothermal and chemotherapy. *Biomaterials*. 2014;35(36):9678–9688. doi:10.1016/j.biomaterials.2014.08.013
23. Farahavar G, Abolmaali SS, Nejatollahi F, et al. Single-chain antibody-decorated Au nanocages@liposomal layer nanoprobes for targeted SERS imaging and remote-controlled photothermal therapy of melanoma cancer cells. *Mater Sci Eng C Mater Biol Appl*. 2021;124:112086. doi:10.1016/j.msec.2021.112086
24. Wu JT, Zhang J, Deng C, Meng FH, Cheng R, Zhong ZY. Robust, responsive, and targeted PLGA anticancer nanomedicines by combination of reductively cleavable surfactant and covalent hyaluronic acid coating. *ACS Appl Mater Interf*. 2017;9(4):3985–3994. doi:10.1021/acsami.6b15105
25. Liu R, Xiao W, Hu C, Xie R, Gao HL. Theranostic size-reducible and no donor conjugated gold nanocluster fabricated hyaluronic acid nanoparticle with optimal size for combinational treatment of breast cancer and lung metastasis. *J Controlled Release*. 2018;278:127–139. doi:10.1016/j.jconrel.2018.04.005
26. C-MJ H, Fang RH, Wang K-C, et al. Nanoparticle biointerfacing by platelet membrane cloaking. *Nature*. 2015;526(7571):118–121. doi:10.1038/nature15373
27. Jiang Q, Luo Z, Men Y, et al. Red blood cell membrane-camouflaged melanin nanoparticles for enhanced photothermal therapy. *Biomaterials*. 2017;143:29–45. doi:10.1016/j.biomaterials.2017.07.027
28. Dash P, Piras AM, Dash M. Cell membrane coated nanocarriers - an efficient biomimetic platform for targeted therapy. Review. *J Controlled Release*. 2020;327:546–570. doi:10.1016/j.jconrel.2020.09.012
29. Liu Y, Wang X, Ouyang B, et al. Erythrocyte-platelet hybrid membranes coating polypyrrol nanoparticles for enhanced delivery and photothermal therapy. *J Mater Chem B*. 2018;6(43):7033–7041. doi:10.1039/c8tb02143k
30. Rosu A, Ghaemi B, Bulte JWM, Shakeri-Zadeh A. Tumor-tropic trojan horses: using mesenchymal stem cells as cellular nanotheranostics. Review. *Theranostics*. 2024;14(2):571–591. doi:10.7150/thno.90187
31. Yun WS, Shim MK, Lim S, et al. Mesenchymal stem cell-mediated deep tumor delivery of gold nanorod for photothermal therapy. *Nanomaterials*. 2022;12(19):3410. doi:10.3390/nano12193410
32. Xu LN, Wang XD, Wang RX, Liu SJ, Xu M. Engineered macrophages: a safe-by-design approach for the tumor targeting delivery of Sub-5 nm gold nanoparticles. *Small*. 2023;19(1):2205474. doi:10.1002/smll.202205474
33. Debele TA, Yu LY, Yang CS, Shen YA, Lo CL. pH- and GSH-sensitive hyaluronic acid-MP conjugate micelles for intracellular delivery of doxorubicin to colon cancer cells and cancer stem cells. *Biomacromolecules*. 2018;19(9):3725–3737. doi:10.1021/acs.biomac.8b00856
34. Xu WJ, Qian JM, Hou GH, et al. A dual-targeted hyaluronic acid-gold nanorod platform with triple-stimuli responsiveness for photodynamic/photothermal therapy of breast cancer. *Acta Biomaterialia*. 2019;83:400–413. doi:10.1016/j.actbio.2018.11.026
35. Joseph MM, Ramya AN, Vijayan VM, et al. Targeted theranostic nano vehicle endorsed with self-destruction and immunostimulatory features to circumvent drug resistance and wipe-out tumor reinitiating cancer stem cells. *Small*. 2020;16(38):2003309. doi:10.1002/smll.202003309

36. Li WJ, Zheng CF, Pan ZY, et al. Smart hyaluronidase-actived theranostic micelles for dual-modal imaging guided photodynamic therapy. *Biomaterials*. 2016;101:10–19. doi:10.1016/j.biomaterials.2016.05.019
37. Li Y, Le TMD, Bui QN, Yang HY, Lee DS. Tumor acidity and CD44 dual targeting hyaluronic acid-coated gold nanorods for combined chemo- and photothermal cancer therapy. *Carbohydrate Polymers*. 2019;226:115281. doi:10.1016/j.carbpol.2019.115281
38. Zhang J, Pan T, Lee J, et al. Enabling tumor-specific drug delivery by targeting the Warburg effect of cancer. *Cell Rep Med*. 2025;6(1):101920. doi:10.1016/j.xcrm.2024.101920
39. Dash SR, Das C, Das B, et al. Near infrared-responsive quinacrine-gold hybrid nanoparticles deregulate HSP-70/P300-mediated H3K14 acetylation in ER/PR+ breast cancer stem cells. *Nanomedicine*. 2024;19(7):581–596. doi:10.2217/nnm-2023-0269
40. Xu X, Zhuang X, Yu H, et al. FSH induces EMT in ovarian cancer via ALKBH5-regulated Snail m6A demethylation. *Theranostics*. 2024;14 (5):2151–2166. doi:10.7150/thno.94161
41. Wahab R, Kaushik N, Khan F, et al. Gold quantum dots impair the tumorigenic potential of glioma stem-like cells via β-catenin downregulation in vitro. *Int J Nanomed*. 2019;14:1131–1148. doi:10.2147/ijn.S195333
42. Nambiar SS, Ghosh SS, Kaur Saini G. Targeted delivery of gliotoxin-loaded nanocarriers heightens therapeutic potential in hypoxic environment of triple-negative breast cancer cells. *ACS Appl Bio Mater*. 2025;8(8):7306–7321. doi:10.1021/acsabm.5c00989
43. Ghanbari-Movahed M, Varnamkhasti BS, Shourian M. Inhibiting Notch activity in breast cancer stem cells by functionalized gold nanoparticles with gamma-secretase inhibitor DAPT and vitamin C. *Chemical Papers*. 2022;76(2):1157–1170. doi:10.1007/s11696-021-01936-w
44. Melamed JR, Ioele SA, Hannum AJ, Ullman VM, Day ES. Polyethylenimine-spherical nucleic acid nanoparticles against gli1 reduce the chemoresistance and stemness of glioblastoma cells. Article. *Mol Pharm*. 2018;15(11):5135–5145. doi:10.1021/acs.molpharmaceut.8b00707
45. Hu K, Zhou H, Liu Y, et al. Hyaluronic acid functional amphipathic and redox-responsive polymer particles for the co-delivery of doxorubicin and cyclopamine to eradicate breast cancer cells and cancer stem cells. *Nanoscale*. 2015;7(18):8607–8618. doi:10.1039/c5nr01084e
46. Kaushik NK, Kaushik N, Yoo KC, et al. Low doses of PEG-coated gold nanoparticles sensitize solid tumors to cold plasma by blocking the PI3K/AKT-driven signaling axis to suppress cellular transformation by inhibiting growth and EMT. *Biomaterials*. 2016;87:118–130. doi:10.1016/j.biomaterials.2016.02.014
47. Saha D, Talukdar D, Mukherjee P, et al. Green synthesis of gold nano-particles using Madhuca indica flower extract and their anticancer activity on head and neck cancer: characterization and mechanistic study. *Eur J Pharm Biopharm*. 2025;207:114625. doi:10.1016/j.ejpb.2025.114625
48. Pan YW, Ma XH, Liu C, et al. Retinoic acid-loaded dendritic polyglycerol-conjugated gold nanostars for targeted photothermal therapy in breast cancer stem cells. *ACS Nano*. 2021;15(9):15069–15084. doi:10.1021/acsnano.1c05452
49. Huai Y, Zhang Y, Xiong X, Das S, Bhattacharya R, Mukherjee P. Gold nanoparticles sensitize pancreatic cancer cells to gemcitabine. *Cell Stress*. 2019;3(8):267–279. doi:10.15698/cst2019.08.195
50. Agarwalla P, Mukherjee S, Sreedhar B, Banerjee R. Glucocorticoid receptor-mediated delivery of nano gold-withaferin conjugates for reversal of epithelial-to-mesenchymal transition and tumor regression. *Nanomedicine*. 2016;11(19):2529–2546. doi:10.2217/nnm-2016-0224
51. Dhanwal V, Katoch A, Nayak D, et al. Benzimidazole-based organic-inorganic gold nanohybrids suppress invasiveness of cancer cells by modulating EMT signaling cascade. *ACS Appl Bio Mater*. 2021;4(1):470–482. doi:10.1021/acsabm.0c00970
52. Gaiser AK, Hafner S, Schmiech M, et al. Gold nanoparticles with selective antileukemic activity in vitro and in vivo target mitochondrial respiration. *Adv Therapeutics*. 2019;2(6):1800149. doi:10.1002/adtp.201800149
53. He H, Liu L, Zhang S, et al. Smart gold nanocages for mild heat-triggered drug release and breaking chemoresistance. *J Control Release*. 2020;323:387–397. doi:10.1016/j.jconrel.2020.04.029
54. Wang J, Zhao H, Song W, et al. Gold nanoparticle-decorated drug nanocrystals for enhancing anticancer efficacy and reversing drug resistance through chemo-/photothermal therapy. *Mol Pharm*. 2022;19(7):2518–2534. doi:10.1021/acs.molpharmaceut.2c00150
55. Li B, Xu Q, Li X, Zhang P, Zhao X, Wang Y. Redox-responsive hyaluronic acid nanogels for hyperthermia- assisted chemotherapy to overcome multidrug resistance. *Carbohydr Polym*. 2019;203:378–385. doi:10.1016/j.carbpol.2018.09.076
56. Liu GE, Tian XR, Shen RY, et al. Double metal nanoparticles loaded and NIR/pH dual responsive drug nanocrystals inhibit cancer stem cells in a multi-modal manner. *Appl Mater Today*. 2024;39:102272. doi:10.1016/j.apmt.2024.102272
57. Zhang W, Jiang Y, Liu L, et al. Implantable microneedles loaded with nanoparticles surface engineered escherichia coli for efficient eradication of triple-negative breast cancer stem cells. *Nano Lett*. 2025;25(5):2041–2051. doi:10.1021/acs.nanolett.4c06052
58. Jiao Y, Wang H, Wang H, et al. A DNA origami-based enzymatic cascade nanoreactor for chemodynamic cancer therapy and activation of antitumor immunity. *Sci Adv*. 2025;11(2):eadr9196. doi:10.1126/sciadv.adr9196
59. Wang XQ, Liu C, Chen XY, et al. A smart nitric oxide (NO) generating immuno-trimetallic nanocatalyst triggering chemodynamic therapy in breast cancer treatment. *Adv Funct Mater*. 2024;34(32). doi:10.1002/adfm.202316186
60. Van de Walle A, Figuerola A, Espinosa A, Abou-Hassan A, Estrader M, Wilhelm C. Emergence of magnetic nanoparticles in photothermal and ferroptotic therapies. Review. *Materials Horizons*. 2023;10(11):4757–4775. doi:10.1039/d3mh00831b
61. Chittineedi P, Mohammed A, Abdul Razab MKA, Mat Nawi N, Pandrangi SL. Polyherbal formulation conjugated to gold nanoparticles induced ferroptosis in drug-resistant breast cancer stem cells through ferritin degradation. *Front Pharmacol*. 2023;14:1134758. doi:10.3389/fphar.2023.1134758
62. Dhandapani S, Samad A, Liu Y, et al. Coprisin/Compound K conjugated gold nanoparticles induced cell death through apoptosis and ferroptosis pathway in adenocarcinoma gastric cells. *ACS Omega*. 2024;9(24):25932–25944. doi:10.1021/acsomega.4c00554
63. Zhao Y, Zhao W, Lim YC, Liu T. Salinomycin-loaded gold nanoparticles for treating cancer stem cells by ferroptosis-induced cell death. *Mol Pharm*. 2019;16(6):2532–2539. doi:10.1021/acs.molpharmaceut.9b00132
64. Marrache S, Dhar S. The energy blocker inside the power house: mitochondria targeted delivery of 3-bromopyruvate. *Chem Sci*. 2015;6 (3):1832–1845. doi:10.1039/c4sc01963f
65. Pan YW, Zhou SQ, Liu C, et al. Dendritic polyglycerol-conjugated gold nanostars for metabolism inhibition and targeted photothermal therapy in breast cancer stem cells. *Adv Healthc Mater*. 2022;11(8):2102272. doi:10.1002/adhm.202102272
66. Chen S, Lei Q, Qiu WX, et al. Mitochondria-targeting "Nanoheater" for enhanced photothermal/chemo-therapy. *Biomaterials*. 2017;117:92–104. doi:10.1016/j.biomaterials.2016.11.056
67. Fan RR, Chen CL, Hu JS, et al. Multifunctional gold nanorods in low-temperature photothermal interactions for combined tumor starvation and RNA interference therapy. *Acta Biomaterialia*. 2023;159:324–337. doi:10.1016/j.actbio.2023.01.036

68. Liu YY, Huang Y, Lu P, et al. Manganese dioxide/gold-based active tumor targeting nanoprobes for enhancing photodynamic and low-temperature-photothermal combination therapy in lung cancer. *ACS Appl Mater Interf*. 2023;15(47):54207–54220. doi:10.1021/acsami.3c06535
69. Mishra SK, Dhadve AC, Mal A, et al. Photothermal therapy (PTT) is an effective treatment measure against solid tumors which fails to respond conventional chemo/radiation therapies in clinic. *Biomater Adv*. 2022:143213153. doi:10.1016/j.bioadv.2022.213153
70. Shahabad ZA, Avci CB, Bani F, et al. Photothermal effect of albumin-modified gold nanorods diminished neuroblastoma cancer stem cells dynamic growth by modulating autophagy. *Sci Rep*. 2022;12(1):11774. doi:10.1038/s41598-022-15660-2
71. Dash SR, Chatterjee S, Sinha S, et al. NIR irradiation enhances the apoptotic potentiality of quinacrine-gold hybrid nanoparticles by modulation of HSP-70 in oral cancer stem cells. *Nanomedicine*. 2022;40:102502. doi:10.1016/j.nano.2021.102502
72. Mîndrilă I, Osman A, Mîndrilă B, Predoi MC, Mihaiescu DE, Buteică SA. Phenotypic switching of B16F10 melanoma cells as a stress adaptation response to Fe3O4/salicylic acid nanoparticle therapy. *Pharmaceuticals*. 2021;14(10):1007. doi:10.3390/ph14101007
73. Mihaliak AM, Gilbert CA, Li L, et al. Clinically relevant doses of chemotherapy agents reversibly block formation of glioblastoma neurospheres. *Cancer Lett*. 2010;296(2):168–177. doi:10.1016/j.canlet.2010.04.005
74. Qu Y, Cui J, Wu Z, et al. Mechano-regulation of cancer cell memory in tumor progression and therapy. *Mechanobiol Med*. 2026;4(1):100165. doi:10.1016/j.mbm.2025.100165
75. Lou FN, Wei QX, Yin YX, et al. CD44-targeted gold-nanorod-based nano-adjuvant combining mild photothermal therapy and immune activation for triple-negative breast cancer therapy. *Acs Appl Nano Mater*. 2025;8(32):16040–16052. doi:10.1021/acsanm.5c02778
76. Dai J, Li J, Zhang Y, et al. GM-CSF augmented the photothermal immunotherapeutic outcome of self-driving gold nanoparticles against a mouse CT-26 colon tumor model. *Biomater Res*. 2023;27(1):105. doi:10.1186/s40824-023-00430-6
77. Ye J, Yu J, Zhao M, et al. Galloyl-boosted gold nanorods: unleashing personalized cancer immunotherapy potential. *J Colloid Interface Sci*. 2025;678(Pt C):272–282. doi:10.1016/j.jcis.2024.09.100
78. Kalyane D, Polaka S, Vasdev N, Tekade RK. CD44-receptor targeted gold-doxorubicin nanocomposite for pulsatile chemo-photothermal therapy of triple-negative breast cancer cells. *Pharmaceutics*. 2022;14(12):2734). doi:10.3390/pharmaceutics14122734
79. Emami F, Pathak S, Nguyen TT, et al. Photoimmunotherapy with cetuximab-conjugated gold nanorods reduces drug resistance in triple negative breast cancer spheroids with enhanced infiltration of tumor-associated macrophages. *J Controlled Release*. 2021;329:645–664. doi:10.1016/j.jconrel.2020.10.001
80. Kiran A, Kumari GK, Krishnamurthy PT, Khaydarov RR. Tumor microenvironment and nanotherapeutics: intruding the tumor fort. Review. *Biomater Sci*. 2021;9(23):7667–7704. doi:10.1039/d1bm01127h
81. Nicolás-Boluda A, Vaquero J, Laurent G, et al. Photothermal depletion of cancer-associated fibroblasts normalizes tumor stiffness in desmoplastic cholangiocarcinoma. *Acs Nano*. 2020;14(5):5738–5753. doi:10.1021/acsnano.0c00417
82. Mulens-Arias V, Balfourier A, Nicolás-Boluda A, Carn F, Gazeau F. Disturbance of adhesomes by gold nanoparticles reveals a size- and cell type-bias. *Biomater Sci*. 2019;7(1):389–408. doi:10.1039/c8bm01267a
83. Ghafarkhani M, Avci CB, Rahbarghazi R, et al. Mild hyperthermia induced by gold nanorods acts as a dual-edge blade in the fate of SH-SY5Y cells via autophagy. *Sci Rep*. 2021;11(1):23984. doi:10.1038/s41598-021-02697-y
84. Arellano L, Villar-álvarez E, Cambón A, et al. Surface-engineered gold nanorods for targeted delivery of PD-L1 siRNA and cancer chemo-phototherapy. *Nanoscale*. 2025;17(44):25537–25554. doi:10.1039/d5nr02667a
85. Zhao J, Wallace M, Melancon MP. Cancer theranostics with gold nanoshells. Review. *Nanomedicine*. 2014;9(13):2041–2057. doi:10.2217/nnm.14.136
86. Honda K, Hishiki T, Yamamoto S, et al. On-tissue polysulfide visualization by surface-enhanced Raman spectroscopy benefits patients with ovarian cancer to predict post-operative chemosensitivity. *Redox Biol*. 2021;41:101926. doi:10.1016/j.redox.2021.101926
87. Qi GH, Zhang Y, Xu SP, et al. Nucleus and mitochondria targeting theranostic plasmonic surface-enhanced raman spectroscopy nanoprobes as a means for revealing molecular stress response differences in hyperthermia cell death between cancerous and normal cells. *Analytical Chemistry*. 2018;90(22):13356–13364. doi:10.1021/acs.analchem.8b03034
88. Hu F, Zhang Y, Chen GC, Li CY, Wang QB. Double-walled Au Nanocage/SiO2 nanorattles: integrating SERS imaging, drug delivery and photothermal therapy. *Small*. 2015;11(8):985–993. doi:10.1002/smll.201401360
89. Lopes J, Ferreira-Gonçalves T, Figueiredo IV, et al. Proof-of-concept study of multifunctional hybrid nanoparticle system combined with nir laser irradiation for the treatment of melanoma. *Biomolecules*. 2021;11(4):511. doi:10.3390/biom11040511
90. Sharifi M, Attar F, Saboury AA, et al. Plasmonic gold nanoparticles: optical manipulation, imaging, drug delivery and therapy. Review. *J Controlled Release*. 2019;311:170–189. doi:10.1016/j.jconrel.2019.08.032
91. Zarska M, Sramek M, Novotny F, et al. Biological safety and tissue distribution of (16-mercaptohexadecyl) trimethylammonium bromide-modified cationic gold nanorods. *Biomaterials*. 2018;154:275–290. doi:10.1016/j.biomaterials.2017.10.044
92. Allami P, Heidari A, Rezaei N. The role of cell membrane-coated nanoparticles as a novel treatment approach in glioblastoma. *Front Mol Biosci*. 2022;9:1083645. doi:10.3389/fmolb.2022.1083645
93. Zhang J, Tao S, Yang J, et al. Cell membrane-coated nanoparticles target multiorgan crosstalk in cardiovascular-kidney-metabolic syndrome. *Acta Biomater*. 2026;213:1–20. doi:10.1016/j.actbio.2026.01.029
94. Lopes D, Lopes J, Serpico L, Santos HA, Paiva-Santos AC. Harnessing nature's blueprint: unlocking the potential of subcellular structure membrane-coated nanosystems for precision medicine. *Bioact Mater*. 2026;57:551–577. doi:10.1016/j.bioactmat.2025.11.015
95. Xu S, Yang H, Minev B, Ma W. Biomimetic and personalized nanovaccines in cancer immunotherapy: design innovations, translational challenges, and future directions. *J Adv Res*. 2026. doi:10.1016/j.jare.2026.01.070